

Aldona Jelińska

Evaluation of ligand-macromolecule interaction

*Supervisors: prof. dr hab. Robert Hołyst,
dr hab. Renata Małgorzata Gadzała-Kopciuch, prof. UMK*

The presented dissertation was prepared within
the International Doctoral Studies at the
Institute of Physical Chemistry of the Polish Academy of Sciences
Department of Soft Condensed Matter and Fluids
Kasprzaka 44/52, 01-224 Warsaw, Poland.



A-21-3, A-21-7, K-g-176, K-g-185, K-k-216, K-k-216

Warsaw, April 2016

K-g-186, K-l-235

Biblioteka Instytutu Chemii Fizycznej PAN

F-B.490/16



9000000163867



B. 490/16

Acknowledgements

At first I would like to thank my supervisor, Prof. Robert Hołyst, for the patient guidance, encouragement and advice he has provided throughout my time as his student.

I would also like to express my gratitude to dr hab. Renata Małgorzata Gadzała-Kopciuch, prof. UMK for her willingness to act as my auxiliary supervisor.

I would like to thank all colleagues from Department III for help and creating great atmosphere in work.

Finally, I would like to thank my family, especially my husband for support and motivation.

Additionally, I would like to thank the National Science Center for funding the project from the funds granted on the basis of the decision number: UMO-2012/07/B/ST4/01400 (Opus 4).

List of papers

- 1.** Lewandrowska, A.; Majcher, A.; Ochab-Marcinek, A.; Tabaka, M.; Hołyst, R. *Anal. Chem.* **2013**, 85, 4051-4056.
- 2.** Majcher, A.; Lewandrowska, A.; Herold, F.; Stefanowicz, J.; Słowiński, T.; Mazurek, A.P.; Wieczorek, S.A.; Hołyst, R. *Anal. Chim. Acta* **2014**, 855, 51-59.
- 3.** Xuzhu Zhang, Andrzej Poniewierski, Aldona Jelińska, Anna Lewandrowska, Stefan A. Wieczorek, Sen Hou, Robert Hołyst; "Evaluating the Equilibrium and Rate Constants of Noncovalent Interactions by Fluorescence Correlation Spectroscopy" to *Soft Matter* (to be submitted)
- 4.** Anna Lewandrowska, Aldona Jelińska, Agnieszka Wiśniewska, Marcin Górecki, Jadwiga Frelek and Robert Hołyst; "Taylor Dispersion Analysis for studying denaturation of proteins by surfactants" to *Analytical Chemistry* (to be submitted)

List of patent and patent applications

Patent application P-400322 - Anna Lewandrowska, Aldona Majcher, Marcin Tabaka, Anna Ochab-Marcinek, Robert Hołyst „Sposób wykrywania powstawania kompleksów pomiędzy makromolekułą a ligandem” (Poland)

Patent P-407087 – Aldona Majcher, Anna Lewandrowska, Robert Hołyst „Sposób wyznaczania współczynników dyfuzji substancji chemicznych w buforze Tris” (Poland)

Thesis

The noncovalent binding of molecules in solutions is important in chemistry, biology, pharmacy, medicine etc. because many different systems, such as proteins with drug, DNA with drug, DNA with proteins, antibodies with antigens etc., form complexes. Determination of the association constant for complex formation is of great importance in the analysis of their interaction. Studies of drug interactions with plasma protein are an element of discovery of new generations of drugs. Binding of drugs to plasma proteins is a very important process in establishing pharmacodynamics and pharmacokinetic properties of drugs, because free drug molecules are more likely to cross the blood-brain barrier and exert pharmacological effect. The association constants can be determined by a variety of methods including equilibrium dialysis, ultrafiltration, ultracentrifugation, flow injection gradient method and electrophoresis. All these methods have some advantages. Yet despite their benefits, they have certain drawbacks, and therefore new methods are needed. **The purpose of my work was to develop a method more precise, faster and more flexible than the others.** In my work I was inspired by the scientific paper by Bielejewska, A., et al. published in *Analytical Chemistry* in **2010**.

In my dissertation, I present a flow injection method in a long, thin and coiled capillary used to determine the association constant for complexes formed by various substances. The method is based on the determination of the width of the concentration distribution of compounds forming complexes. The study involves mostly drug-protein complexes. In my experiments I used Bovine Serum Albumin (BSA) as a model plasma protein. I determined the association constants of a large number of drugs with BSA. I also

determined the value of the association constants of the complexes of albumin with 3 β - and 3 α - aminotropane derivatives (potential drugs). The compounds were obtained during a search for a new generation of antipsychotics. Additionally, I present two variants of the flow injection technique. In one of them protein and drugs are injected into the protein solution which has a constant protein concentration. In the second method the ligand-macromolecule is injected into pure buffer and the protein concentration is not constant. Finally, I apply our method to study the formation of dye-micelle and protein-DNA complexes.

Table of contents

Thesis	4
Table of contents	6
Abbreviations and symbols	9
1. Introduction	13
1.1 Fundamental interactions: interactions in physics.	13
1.2 Effective interactions in chemistry	14
1.2.1 Non-specific interactions	14
1.2.2 Specific interactions – formation of the ligand–macromolecule complexes.	19
1.3 Stoichiometry of a complex.	21
1.4 Binding to a single site.	23
2. Experimental methods	25
2.1 Equilibrium dialysis.	26
2.2 Ultrafiltration.	30
2.3 Ultracentrifugation.	30
2.4 Capillary electrophoresis: the method basics.	31
2.4.1 Affinity Capillary Electrophoresis.	34
2.5 Flow Injection Analysis: theoretical basis of the method.	35
2.5.1 Flow injection gradient method.	38
3. A new perspective of determination of the association constant by flow injection method: theoretical background	41

3.1 Dispersion in a straight capillary: Taylor dispersion method for determination of the diffusion coefficient.	41
3.2 Dispersion in a coiled capillary.	42
3.3 Straight capillary vs coiled capillary.	44
3.4 Determination of the association constant based on the diffusion coefficient using Flow Injection Method.	45
4. Experimental part.	49
4.1 Chemicals.	49
4.2 Equipment.	51
4.3 Determination of the capillary radius.	52
5. Application of the theory for determination of the association constant by flow injection method.	53
5.1 Drug-protein interactions: a test of the method.	53
5.2 Comparison of association constants obtained at high and low flow rates of a carrier phase.	55
5.3 Application of the method to complexes of BSA with 3 β - and 3 α -aminotropane derivatives.	56
5.4 Technical limitations of the method: range of concentrations and association constants.	60
6. A new perspective of determination of the association constant by flow injection method.	64
6.1 Reduction of the amount of reagents: experimental challenges.	66
6.1.1 Overlapping of peaks.	66
6.1.2 Effective diffusion coefficient in single injection experiment.	67
6.1.3 Changes of macromolecule concentration at different flow rates	68

6.1.4 Changes of the macromolecule concentration.	70
6.1.5 Changes in the concentration of compounds	71
6.1.6 Modifications of the equations	75
7. Surfactant–dye interactions.	77
7.1 Surfactants.	77
7.2 Formation of the micelle-dye complex: theory.	78
7.3 Interactions of rhodamine 110 with cationic surfactant cetyltrimethylammonium chloride (CTAC).	80
7.4 Interactions of atto 488 with anionic surfactant sodium dodecyl sulfate (SDS)	82
8. Protein-DNA interactions.	86
8.1 Protein-DNA interactions: the aim of this work.	86
8.2 Description of the experiment.	87
8.3 Results and conclusions.	89
9. Summary and conclusions.	91
10. References.	94

Abbreviations and symbols

BSA bovine serum albumin

TBP TATA-binding protein

ED equilibrium dialysis

UC ultracentrifugation

UF ultrafiltration

CE capillary electrophoresis

EOF electro-osmotic flow

ACE affinity capillary electrophoresis

FIA flow injection analysis

FIG flow injection gradient method

IRF 9 interferon regulatory factor

U3C cell line

DTT dithiothreitol

CMC critical micelles concentration

PEEK polyether ether ketone

TRIS 2-Amino-2-hydroxymethyl-propane-1,3-diol

ρ density of carrier phase

σ dispersion coefficient

σ_c dispersion coefficient in a coiled capillary

μ electrophoretic mobility

η viscosity

γ viscosity of carrier phase

ε molar extinction coefficient

λ wavelength

Θ the fraction of binding sites on the macromolecule which are occupied by ligand

M macromolecule

L ligand

K_{eq} equilibrium constant

K_a association constant

K_d dissociation constant

R gas constant

T temperature

F the force of gravity

G gravitational constant

M mass of the one object

m mass of the other object

r distance between two objects

ΔG^\ominus Gibbs free energy

ΔH enthalpy

ΔS entropy

k_{on} association rate constant

k_{off} dissociation rate constant

D_{eff} effective diffusion coefficient

D molecular diffusion coefficient

D_L diffusion coefficient of the ligand

D_M diffusion coefficient of the ligand

D_{LM} diffusion coefficient of the complex

D_{dye} diffusion coefficient of free dye

$D_{complex}$ diffusion coefficient of dye-micelle complex

t_L time spent by the ligand in the free state

t_{LM} time spent by the ligand in the bound state

t_T total time from injection to detection point

t_{dye} time spent in the free state

$t_{complex}$ time spent in the bound state

Δt time from injection point to detection point

t^* return time

t time of measurement

c_M macromolecule concentration

F flow rate of carrier phase

u velocity

R radius of the capillary

r external capillary radius

L length of the capillary

v velocity of the ion migration

E electric field

q molecule charge

r ion radius

C_{LM}^{eq} concentration of the complex at equilibrium

C_L^{eq} concentration of the ligand at equilibrium

C_M^{eq} concentration of the macromolecule at equilibrium

$C_{L(initial)}$ concentration of the ligand in the injected sample

C_M^0 overall concentration of the macromolecule

C_0 concentration of the injected sample

C_{max} maximum concentration of the injection

C_m concentration of micelles

C_s surfactant concentration

N_{ag} mean number of aggregated surfactant molecules

S_m micelle

H_0 peak height

H_{max} maximum peak height

1. INTRODUCTION

1.1 Fundamental interactions: interactions in physics

Interaction is a kind of action occurring when two or more objects have an effect upon one another. In physics, a fundamental interaction is a process by which elementary particles interact with each other. Four basic forces are known:

- Gravitational - this is a force that attracts any object with mass. Every object in the universe is pulling toward every other object. This fact is related to the universal law of gravitation, which is called the Newton's law.^{1,2} This law is expressed by the universal gravitation equation:

$$F = \frac{GMm}{r^2} \quad (1.1.1)$$

Where: F [N] is the force of gravity, G is the gravitational constant (6.67×10^{-11}), M [kg] is the mass of one object, m [kg] is the mass of the other object, r [m] is the distance between the two objects. Some corrections of $\frac{1}{r^2}$ law appear in the general theory of relativity.³

- Weak – the weak interaction is responsible for radioactive decay of subatomic particles. Additionally, this force plays a key role in the nuclear reaction process (i.e. nuclear fission).⁴
- Electromagnetic – this is a force that appears between electrically charged particles (i.e. electrons, protons etc.). This fundamental interaction is related to electric force (produced by electric field) and magnetic force. The magnetic

force is a manifestation of the magnetic field created by moving, charged particles.⁵

- Strong – the strong interaction is called the strong force or nuclear strong force. It is responsible for two processes: first, the strong force keeps protons and neutrons in the nucleus of an atom, and second, the strong force connects quarks to form protons and neutrons.⁶

1.2 Effective interactions in chemistry

Effective interactions in chemistry come mostly from fundamental electrostatic interactions. They appear when structures are formed by charged protons and electrons, atoms and compounds. From the chemical point of view, most complexes are formed as a result of non-covalent interactions, which produce dynamic equilibrium between complexes. Generally, non-covalent interactions are divided into two classes:

Non-specific interactions - these interactions influence formation of the complexes, which have not been very well-defined by stoichiometry or which create loosely-bound aggregates (i.e. weak hydrophobic attraction, electrostatic repulsion and attraction, van der Waals potentials, etc.)

Specific interactions - this kind of interactions involves very well-defined complexes with exact stoichiometry such as macromolecule-ligand complexes (i.e. protein-drug complexes, protein-DNA complex).⁷

1.2.1 Non-specific interactions

Van der Waals interaction (van der Waals interaction). This kind of force refers to the attractive and repulsive force between molecules (or between parts of the same

molecule) that are close together in space. Van der Waals interactions play a key role in such fields as condensed matter physics, supramolecular chemistry, nanotechnology, structural biology etc.^{8,9} The Van der Waals forces include:

- ✓ Dipole-dipole interactions (called the Keesom force). They consist of attractive interactions between dipoles that are as a whole averaged over different rotational orientations of the dipoles (Figure 1 A). However, sometimes alike charges are next to one another causing repulsion (Figure 1 B).^{10,11}

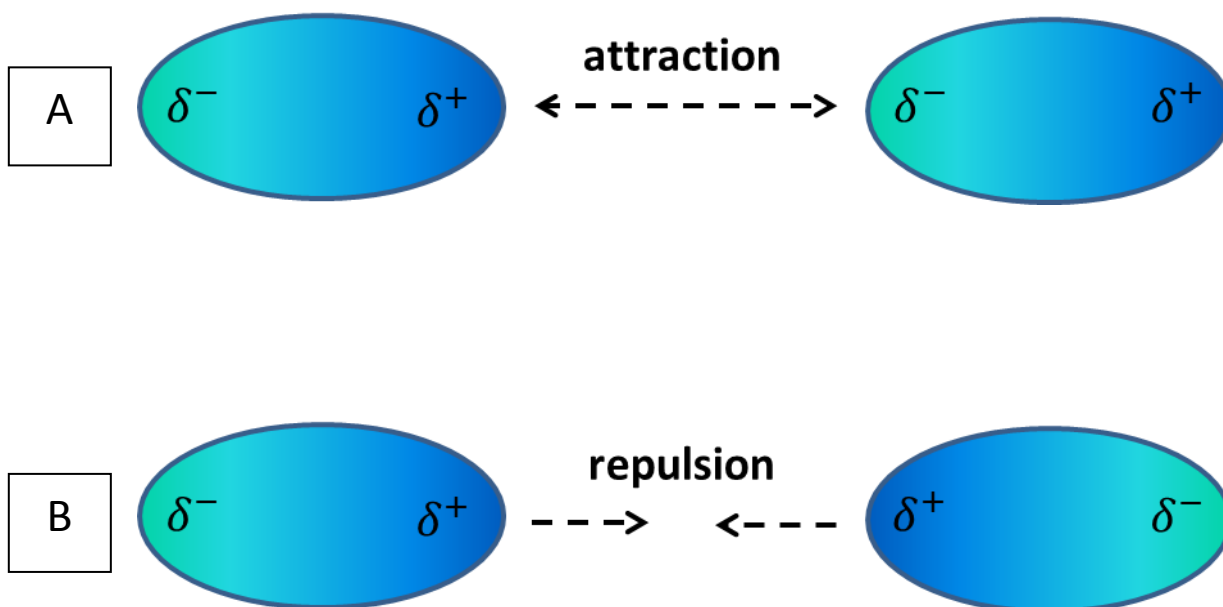


Figure 1. Dipole-dipole electrostatic attraction (A) and repulsion (B).

- ✓ Dipole-induced dipole interactions (known as the Debye force). A molecule with a permanent dipole creates an electrostatic field in its own surroundings. The electrostatic field shifts the electrons of the second molecule (which is close to the first one) and contributes to the creation of induced dipole moment. The induced dipole forces appear from the polarization. The interaction between

dipole and induced dipole occurs between any polar molecule and non-polar or symmetrical molecule.¹²



Figure 2. Dipole-induced dipole interactions. The electrons of the second molecule are attracted by the positive end of the first molecule. As a consequence, the electrons of the second molecule migrate to the left side and make the left side more negative.

- ✓ Induced dipole-induced dipole interaction (called the London dispersion force).

The London interactions are caused by the fluctuations of electron density of a molecule or atom (appearance of instantaneous dipole moment). Therefore, all molecules and atoms are oscillating dipoles. When molecules are close to each other, oscillating dipoles sense each other and create couples. The movements of the electrons in these molecules are correlated. The fluctuating, coupled dipoles sense dispersive interactions. They are always attractive and appear between any pair of molecules, polar or non-polar, which are located in their surroundings.¹³⁻¹⁶

Ionic interactions are a kind of electrostatic interaction. Electrostatic attraction appears between closely located ions that have an opposite charge, while electrostatic repulsion exists between ions that have the same charge. Ionic bonds involve the transfer of electrons between ions, as depicted in the exemplary Figure below:

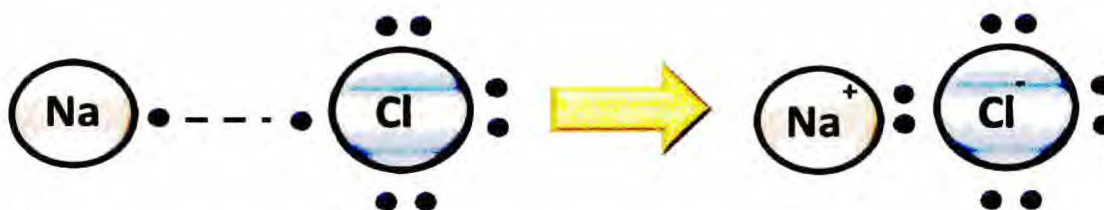


Figure 3. Formation of the ionic bond for sodium chloride.

The main aim of forming chemical bonds is to have an octet (except of Helium, which requires a doublet). Therefore, most atoms have to lose or gain one or two electrons. Ionic bonds help atoms to achieve noble-gas electron configurations (the stable state for an atom). However, pure anionic bonds cannot exist. The strength of an ionic bond depends on the environment of the ionic compound.¹⁷⁻¹⁹

Hydrogen bonding is the Coulombic interaction which involves a hydrogen atom located between two strongly electronegative atoms and binds them together:



Where X and Y mean nitrogen, fluorine or oxygen.

Hydrogen bonds exist between atoms in different molecules or in parts of the same molecule. It has the strength of the order of 20 kJ mol^{-1} . Due to the high number of hydrogen bonds, water is a liquid in a wide temperature range (from $0 \text{ }^\circ\text{C}$ to $100 \text{ }^\circ\text{C}$ at normal pressure). Additionally, the hydrogen bonds take part in the formation of helices and sheets of polypeptide chains and play a part in the folding of the protein.²⁰⁻²²

Hydrophobic interactions describe the interactions between water and low-water soluble molecules (called hydrophobes). As hydrophobes are nonpolar molecules, they

prefer other neutral molecules and non-polar solvents. The classical example of the hydrophobic interaction effect is mixing of fat and water. Why do oil and water not mix? It is related to the thermodynamics of hydrophobic interactions. When a hydrophobe is placed in an aqueous medium, the hydrogen bonds between water molecules are broken (they create a place for the hydrophobe). Water molecules make new hydrogen bonds and can form a clathrate cage around the non-polar molecules. This is a type of endothermic reaction (entropic effect) because the hydrogen bonds were destroyed and heat was put into the system. However, the change of enthalpy, ΔH , can be negative, positive or zero. It depends on how many new hydrogen bonds can compensate for the hydrogen bonds broken by the entrance of the non-polar molecule. In most cases when non-polar molecules interact with each other, enthalpy (ΔH) is positive. On the other hand, the mixing of hydrophobic molecules and water causes an increase in entropy, ΔS , or a decrease during the forming of the clathrate cage. Changes of ΔH , ΔS and the free energy, ΔG (Gibbs energy), are related according to the following formula:

$$\Delta G = \Delta H - T\Delta S \quad (1.1.2)$$

Where T is the temperature of the system.

All chemical reactions are based on changes of free energy, ΔG . Most systems which react at standard conditions of temperature and pressure, achieve a minimum of the free energy. However, by measuring changes in the free energy, ΔG , we are able to define the favorability of a given reaction. When ΔG is negative, the reaction process is favored. This is also related to the fact that the energy will be released from the reaction process. Furthermore when ΔG is positive, the energy (i.e. in the form of work) should be delivered to the system. From the values of ΔH and ΔS (according to Formula 1.1.2) we are able to estimate the spontaneity of the process. Additionally, the change of Gibbs

free energy for reagents in the standard state (demonstrated by θ), ΔG^θ , is an inherent property of reaction and is related to the equilibrium constant, K_{eq} . The relation between K_{eq} and ΔG^θ is as follows:

$$\Delta G^\theta = -RT \ln K_{eq} \quad (1.1.3)$$

Where ΔG^θ is the standard Gibbs free energy change of reaction, R is the gas constant, and T is the absolute temperature.

The equilibrium constant value is independent of the concentrations of the reactants and products included in solution, but depends on temperature and on ionic strength. K_{eq} is a constant for a given set of solution conditions (i.e. temperature, pressure, ionic strength and pH), because the change of free energy, ΔG^θ (Gibbs energy), of binding (i.e. binding of ligand to macromolecule) is a constant for these conditions.²³⁻²⁵

1.2.2 Specific interactions – formation of the ligand-macromolecule complexes

The study of non-covalent binding of a ligand to a macromolecule is based on the measurements of the association constant (also called the equilibrium constant or affinity constant). In general, one or more ligands can bind to a macromolecule.²⁶

A scheme for the formation of the complex 1:1 is as follows:



Where L is the ligand, M is the macromolecule and ML is the complex.

The association constant determines how strongly the molecules are bound. This constant is defined by the following equation:

$$K_a = K_{eq} = \frac{[ML]}{[M][L]} \quad (1.2.2)$$

Where K_{eq} [M^{-1}] is the equilibrium constant of the reaction of the complex formation at equilibrium, $[ML]$ is the equilibrium concentration of the complex, $[M]$ is the equilibrium concentration of the macromolecule, $[L]$ is the equilibrium concentration of the ligand in the system.

The process of the complex formation is reversible and the reversed process is treated as dissociation. At equilibrium the rates of the opposing reactions are equal and the concentrations of the compounds no longer change. Under these conditions the equilibrium concentrations of substrates and products and the rate constants k_{on} and k_{off} will have a constant ratio which gives the value of K_d . Therefore the equation can be written as:

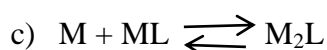
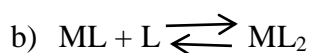
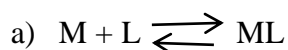
$$K_d = \frac{[M][L]}{[LM]} = \frac{k_{on}}{k_{off}} = \frac{1}{K_a} \quad (1.2.3)$$

Where K_d is dissociation constant, k_{on} is association rate constant, and k_{off} is the dissociation rate constant.

The knowledge of the association constant is essential for understanding many biochemical processes such as oxygen transport (binding of dioxygen to hemoglobin),²⁷ energy production (binding of glycerol-phosphate to triose phosphate isomerase)^{28,29} recognition in the immune system (binding of antibody HyHEL-10 to lysozyme)^{30,31} etc. However, before we can determine the association constant, we must know the exact stoichiometry of the complex.

1.3 Stoichiometry of a complex

In the considerations of simplest complexes, the three different stoichiometries of complex exist: ML, ML₂, M₂L. They are related by the following equilibria:



They are defined by the following stepwise binding constants:

$$\text{a) } K_a = \frac{[ML]}{[M][L]} \quad (1.3.1)$$

$$\text{b) } K_a = \frac{[ML_2]}{[ML][L]} \quad (1.3.2)$$

$$\text{c) } K_a = \frac{[M_2L]}{[M][ML]} \quad (1.3.3)$$

Higher complexes are constructed in this manner. However, we can also write the formation of complexes directly (from ligand and macromolecule):



Thus, to define the overall binding constant we write:

$$K_a = \frac{[M_mL_n]}{[M]^m[L]^n} \quad (1.3.5)$$

Where *m* and *n* are stoichiometric coefficients in M_{*m*}L_{*n*} complex.³²

In general, characterization of the association constant requires information regarding stoichiometric coefficients *m* and *n* in M_{*m*}L_{*n*} complex. The conventional method for determination of stoichiometry is to isolate the saturated complex then break the complex separately and measure (quantitatively) the released moles of components. The next option is to measure the molecular weight of the separated complex and compare

this to an unbound macromolecule. The most popular methods for separating macromolecules are gel filtration,^{33,34} electrophoresis,^{35,36} and differential precipitation.^{37,38} However, in biochemical systems in which we use a typical, small ligand and a large macromolecule it is difficult to observe difference in molecular properties (i.e. electrophoretic mobility, molecular size etc.) of a free and a bound macromolecule. Moreover, it is hard to separate out saturated complexes from the mixture in dynamic equilibrium. Therefore, the evaluation of binding sites and the association constant is based on construction of the models (e.g. one site specific binding model).^{32,39}

There are systems in which the macromolecule (e.g. DNA) have more than one binding site.⁴⁰ However, binding to multiple sites is quite complicated due to the differences between the macroscopic binding constant and microscopic binding constant. The microscopic binding constant, k_m is related to the binding to a specific site, for example binding to one site out of n sites which are situated on the macromolecule (e.g. a DNA strand).⁴¹ Mostly it is the macroscopic value of the binding constant in the experiment that is measured as it is really hard to distinguish different complexes experimentally. Due to this problem and other complications (e.g. cooperative behavior and allosteric interaction), the binding of a ligand to a single binding site on a macromolecule is what is most frequently studied.

The example of one-site binding in biological systems is the binding of a protein to a single DNA binding site. The affinity to a given binding site is given by the dissociation constant. The constant K_d for such a system is in the range from 1 nM to 1 pM for site specific binding to DNA.⁴²⁻⁴⁶

TATA box-binding protein

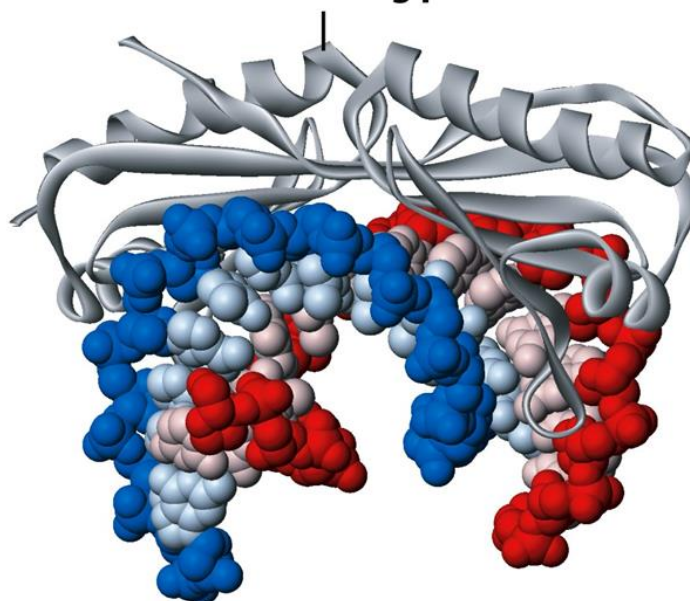


Figure 4. An example of specific one-site binding. The DNA-binding protein is the TATA-binding protein (TBP). It is a transcription factor that binds a specific (strictly defined) sequence in the promoter of eukaryotes.⁴⁷

1.4 Binding to a single site

In the situation, where only one binding site exists per ligand molecule ($n=1$), an equation describing the amount of ligand bound to the macromolecule, or its saturation is given by the relation:

$$\Theta = \frac{[L]_{bound}}{[M]_{total}} = \frac{[LM]}{[M]+[LM]} \quad (1.4.1)$$

Where Θ is the fraction of the ligand-binding sites on the macromolecule which are occupied by the ligand, $[L]_{bound}$ is the concentration of the ligand bound to the macromolecule, and $[M]_{total}$ is the total concentration of the macromolecule.

Determination of Θ requires spectrophotometric (e.g. UV absorbance spectra) manipulation. This manipulation (in experiments) is based on adding a specified

concentration of ligand molecules to a constant concentration of macromolecules. Next, to establish the fraction of the ligand-binding sites on the macromolecule, which are occupied by the ligand, the observation and integration of spectra is needed. After this exercise in spectrophotometric manipulation we can establish the θ .

Establishing θ by UV absorbance spectra is possible in systems which exhibit slow exchange in complex formation. For given θ , we can combine equations 1.2.3 and 1.4.1 and we obtain:

$$\theta = \frac{[L]}{K_d + [L]} \quad (1.4.2)$$

The above relation is fulfilled only if $L_{free} \approx L_{total}$ in the experimental conditions. For binding to a single site the theoretical assumptions consider plotting θ versus $[L]^n$ at a constant concentration of $[M]_{total}$. Next, dependence requires using one site specific binding model.⁴⁸ The graphical representation of dependence (1.4.2) in a shape of hyperbola is known as a Langmuir isotherm:

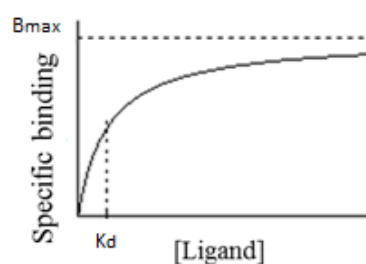


Figure 5. An example of fitting a saturation binding curve. Specific binding signifies the amount of ligand bound to the macromolecule. B_{max} is the maximum amount of the ligand which can bind specifically to the macromolecule. The midpoint of this non-linear binding curve indicates the value of the dissociation constant. K_d corresponds to ligand concentration which occupies 50% of the macromolecule.

However, choosing the midpoint of the hyperbola is difficult, therefore the equation can be changed to the following form:

$$\frac{\theta}{[L]} = \frac{1}{K_d} - \frac{\theta}{K_d} \quad (1.4.3)$$

The graphical representation of the equation (1.4.3) is called the Scatchard plot:

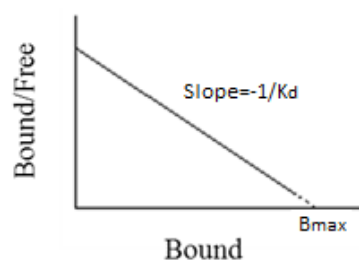


Figure 6. *The Scatchard plot is a binding graph. It presents the ratio of the amount of bound ligand to the amount of free ligand as a function of the amount of ligand bound, Θ . From the slope $-\frac{1}{K_d}$ we can calculate the value of the dissociation constant.*

The Scatchard plot is useful in the typical experimental techniques such as equilibrium dialysis, electrophoresis and fluorescence assay.^{49,50}

2. Experimental methods

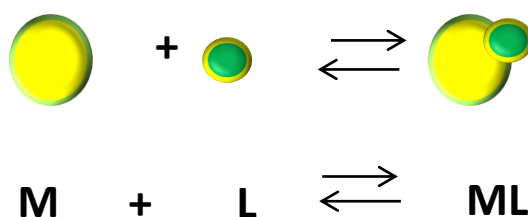
This section will be concerned with the theoretical background of the experimental methods allowing to determine the association constant. At present, there are several

methods used for measurements of the association constant such as equilibrium dialysis, the ultrafiltration process, the ultracentrifugation, affinity capillary electrophoresis and flow injection analysis.

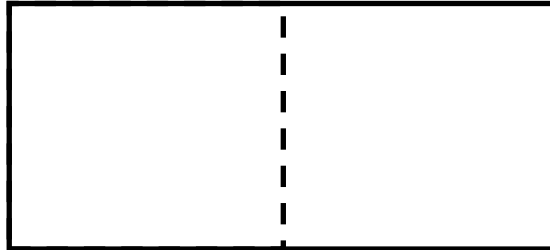
2.1 Equilibrium dialysis

The equilibrium dialysis is the most common method used for determination of the value of the association constant. This separation method is used mainly for the reactions between macromolecules (M) and the ligands (L) differing significantly in size, shape or molecular weight.⁵¹ The method is considered as a reference method especially in pharmaceutical industry. Equilibrium dialysis is also considered as quite accurate, simple and inexpensive technique. It is based on differences in permeability of different molecules through a semipermeable membrane. A system of two types of molecules, initially separated by a semipermeable membrane, is allowed to diffuse and react until the reaction equilibrium is reached. Generally, the amount of a ligand bound to a macromolecule is measured in different experimental conditions. It makes it possible to obtain information on various binding parameters of the samples for example the value of the association constants, binding sites etc. This method allows to analyze formation of many different types of complexes and gives possibility to study low-affinity interactions.⁵²

A typical dialysis with a reaction of association can be described schematically as follows:

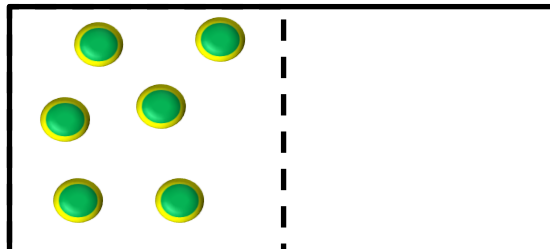


- 1) We have two chambers which are separated by a semipermeable membrane. The selection of the membrane depends on the choice of the macromolecule (M) which interacts with the ligand (L).



Chamber 1 (for assay L) Chamber 2 (for sample M)

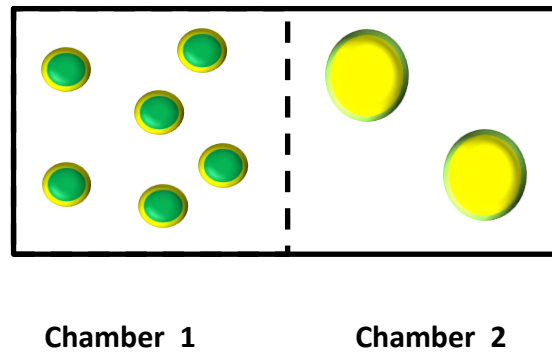
- 2) The molecules of the ligand (of known concentration and volume) are placed in Chamber 1. The ligand, due to its small size, permeates through the semipermeable membrane.



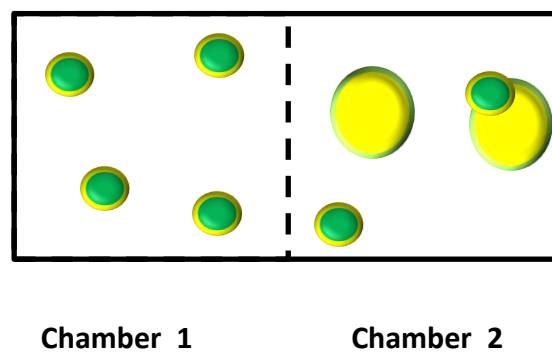
Chamber 1

Chamber 2

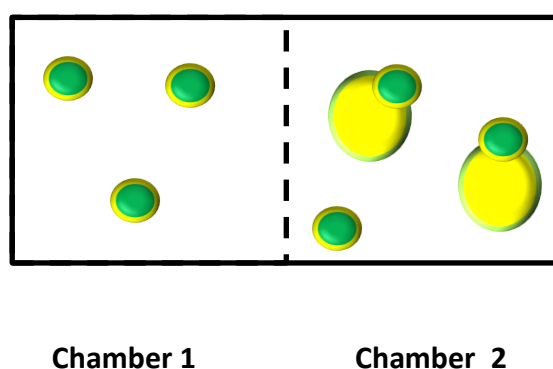
- 3) A volume of known concentration of the macromolecule is placed in the Chamber 2. The volume of the macromolecule should be equivalent to the volume placed in Chamber 1.



- 4) The molecules of the ligand diffuse across the membrane and some of them are bound to the macromolecules. However, partially some molecules diffuse alone in the solution.



- 5) The diffusion of the ligand is continued until the equilibrium of the process is reached. The concentration of the free ligand is the same in both chambers. However, total concentration of the ligand in Chamber 2 is higher because part of the ligand are bound to the macromolecules.



The concentration of the ligand in both chambers is determined experimentally. The overall concentration of the macromolecule is also known. To determine the association constant, the Scatchard plot is needed. This graphical method requires creating a saturation isotherm, fitting the data and using one site binding model (described in subsection 1.4).^{53,54}

Equilibrium dialysis is not a perfect technique. Like most chemical methods, it has numerous disadvantages, the first and very important being the process length (up to 24 h). The time depends here on the choice of the ligand/macromolecule system, which has to reach equilibrium. The second problem is the volume shift in the chambers, as the changes in the volume can be rather significant (10-30%). It is related to the osmotic pressure created due to the semipermeable membrane and to the presence of the

macromolecules. Another phenomenon causing errors is the process of adsorption of the molecules on the walls of the chambers or on the membrane. Because of this, the total concentration can change even by 50%. The last drawback is the Donnan effect (also called Donnan law or Donnan equilibrium) describing the behavior of charged particles near a semi-permeable membrane. This effect disturbs the equilibrium state because of the changes of the electric potential (Donnan potential).^{52,55}

2.2 Ultrafiltration

The next method for determination of the association constant is ultrafiltration. This method is very similar to the equilibrium dialysis as this technique also utilizes special membranes. However, the most important difference lies in application of pressure during the process. Thanks to this operation, the method is faster than the dialysis. Because of the similarity of these two methods, their disadvantages are also almost identical. Ultrafiltration suffers from many drawbacks such as: nonspecific binding of the compounds to the membrane, Donnan effect and protein leakage. Additionally, some authors claim that the application of high pressure during the process has strong influence on the stability of the binding equilibrium.⁵⁶⁻⁵⁸

2.3 Ultracentrifugation

The ultracentrifugation (UC) is an analytical technique which makes it possible to study a complex formation. The solution of ligands and the protein is put in a special tube. All compounds are placed in the centrifugal field at the standard rotating speed of about 60,000 rpm. The process of centrifugation is continued until proteins and complexes sediment to the bottom of the tube (Figure 7).

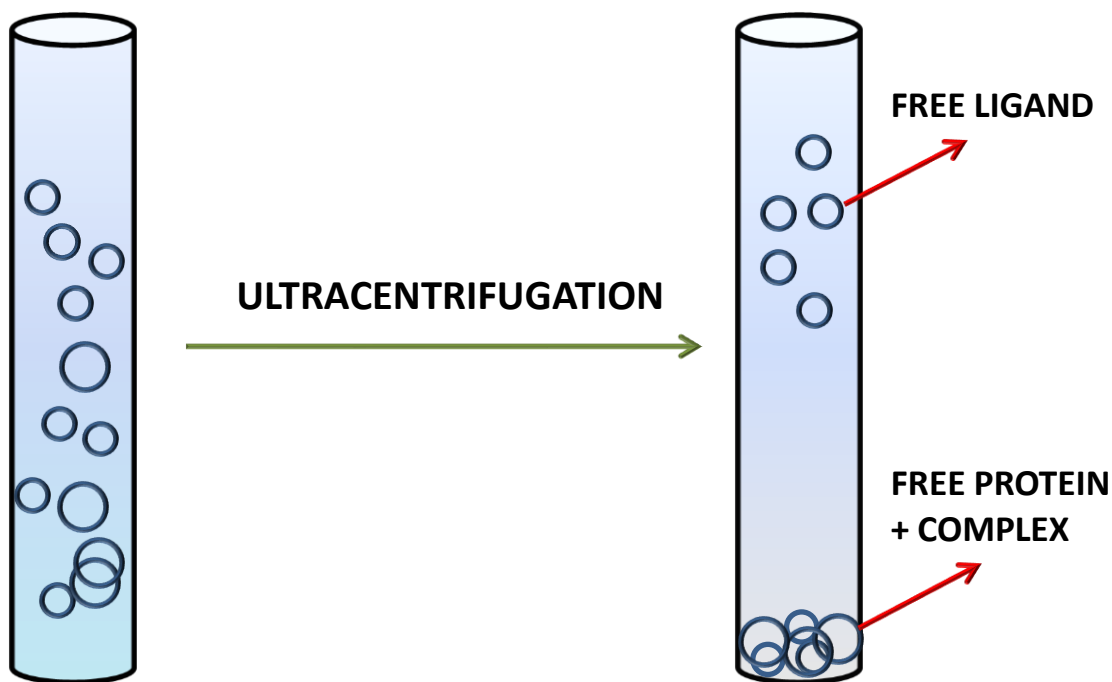


Figure 7. *The process of ultracentrifugation.*

The method allows to eliminate difficulties present in the equilibrium dialysis (ED) and ultrafiltration (UF) such as problems with adsorption on the membrane, Donnan effect, leakage etc. Nevertheless, the main problem with this technique is the estimation of concentration of the free drug fraction. The error is 10-40% and depends on the size of the macromolecules (higher error for larger molecules). The process of determination of the fraction of the free drug can be disturbed by sedimentation process, back diffusion and viscosity. The long, problematic analysis makes ultracentrifugation an unattractive method for studies of intermolecular interactions.⁵⁹⁻⁶¹

2.4 Capillary electrophoresis: the method basics

Capillary Electrophoresis (CE) is a method of separation of ions in a thin (25-100 μ m) capillary. The capillary is made of fused silica, filled with the solution of electrolyte.

The sample is injected into the electrolyte solution from one end of the capillary (opposite to the detector). The ions move under the influence of the high voltage from power supply applied to both electrodes. The ions move towards the detector situated at the opposite end of the capillary. Their motion carries the solution. The detector is connected to the computer for data acquisition.^{62,63}

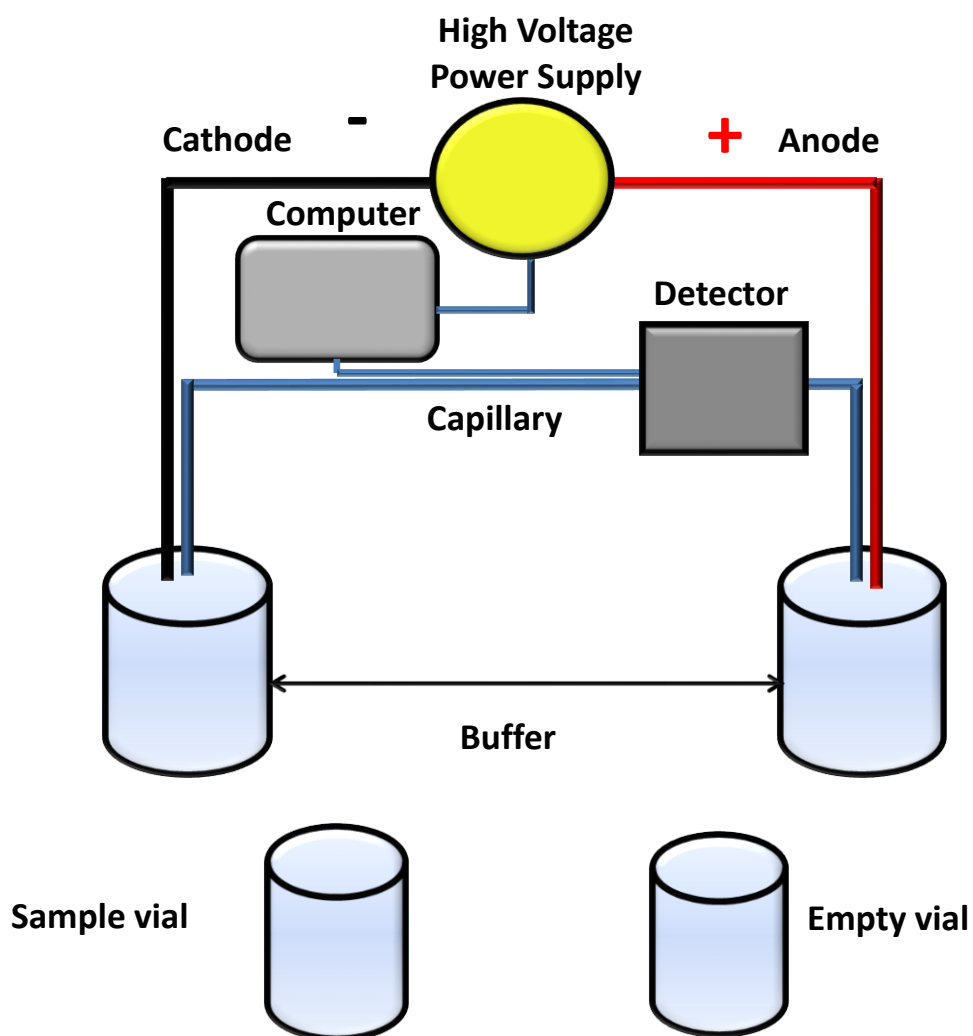


Figure 8. Schematics of the experimental setup in typical capillary electrophoresis.

The ions move under the applied voltage. The basis of the separation of the ions is the difference in mobility of the charged molecules. The velocity [$\text{cm} \cdot \text{s}^{-1}$] of ion migration depends on electrophoretic mobility and applied voltage:

$$v = \mu E \quad (2.4.1)$$

Where E [V/cm] is the electric field and μ is the electrophoretic mobility described as follows:

$$\mu = \left(\frac{q}{6\pi\eta r} \right) \quad (2.4.2)$$

Where q [C] is the charge of the molecule, η [Pa·s] is the viscosity [$\text{kg} \cdot \text{m}^{-1} \cdot \text{s}^{-1}$] of the solution, and r [m] is a radius of the ion.

Relation 2.4.2 shows that if two ions are the same size, the one with greater charge will move faster. Also the smaller ion will be faster than the larger one with the same charge.

The flow inside the capillary (filled with buffer solution) is called electro-osmotic flow (EOF). It occurs because of presence of electrical double layer on the interphase between the solution and the capillary walls. At high values of pH the groups of fused silica have negative charge and they attract cations of the electrolyte (ionization of the capillary wall). The cations are solvated by molecules of the solvent and they move together with all molecules in the solution. The velocity of the electro-osmotic flow is usually higher than the velocity of the ion migration. As a result, cations, anions and neutral molecules move towards the cathode (-).⁶⁴

Consequently, the velocity of migrating ions decreases in a following sequence: the fastest are small cations with high charge, slower are large cations with smaller charge,

certain neutral molecules, large anions with small charges and the slowest are small anions with high charge, as depicted in Figure 9.

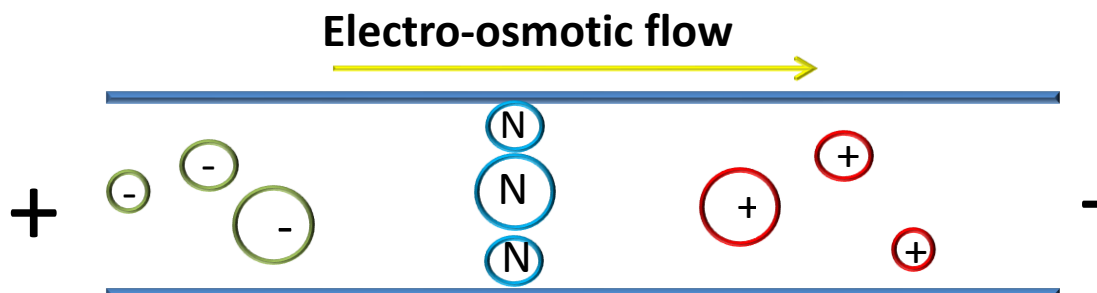


Figure 9. The sequence of migration velocity of different ions. The arrow indicates the direction of the electro-osmotic flow.

To determine the association constant for ligand-macromolecule systems, the Affinity Capillary Electrophoresis is used.⁶⁵

2.4.1 Affinity Capillary Electrophoresis

The affinity capillary electrophoresis (ACE) is a technique that is used to measure the binding affinity of macromolecules to charged and uncharged ligands (the basics of the technique are described in section 2.4). In this type of electrophoresis, the electrophoretic mobility is measured for free and bound macromolecules. ACE measures the electrophoretic mobility for a macromolecule as a function of concentration of the ligand.

In the first case the binding constant is determined from the equations:

$$\frac{\Delta\mu_{M,L}}{[L]} = K_a \Delta\mu_{M,L}^{max} - K_a \Delta\mu_{M,L} \quad (2.4.1)$$

or

$$\frac{\Delta t_L}{[L]} = K_a \Delta t^{max} - K_a \Delta t_L \quad (2.4.2)$$

where K_a is the association constant, $\Delta\mu_{M,L}$ is the change of the electrophoretic mobility of the macromolecule M for chosen concentration of the ligand [L] ($\Delta\mu_{M,L} = \mu_{M,L} - \mu_M$), and $\Delta\mu_{M,L}^{max}$ is the change of the electrophoretic mobility at a concentration of ligand that will saturate the active site of the macromolecule. We assume that the differences in electrophoretic mobility in Eq. 2.4.1. can be replaced by the differences in migration time. These assumptions lead to Eq. 2.4.2 and make it possible to determine the binding constant.

The ACE can be used for determination of interactions between a macromolecule and charged and neutral ligands. The main drawback of ACE is the fact that the ligand can change the electrophoretic mobility of the macromolecule during the creation of the complex. Additionally, adsorption in the capillary is still a problem. Due to that certain systems cannot be studied using ACE method.^{65,66}

2.5 Flow Injection Analysis: theoretical basis of the method

Flow injection analysis (FIA) is a technique in which sample dispersion in a carrier phase is considered. A sample is injected into a stream of solution and it forms a well-defined sample zone. The flow leads to the flow-induced widening of the initially narrow injection zone of the analyte. The sample disperses into the carrier stream and forms the concentration gradient. When the sample moves through the mixing chamber (reaction zone), the width of its flow profile increases. In this way there is a possibility to monitor the product of a chemical reaction between the sample and the reactant. The final profile of the product is collected by optical or electrochemical detectors. The FIA curve is a plot of the detector's signal as a function of time, as depicted in Figure 10.

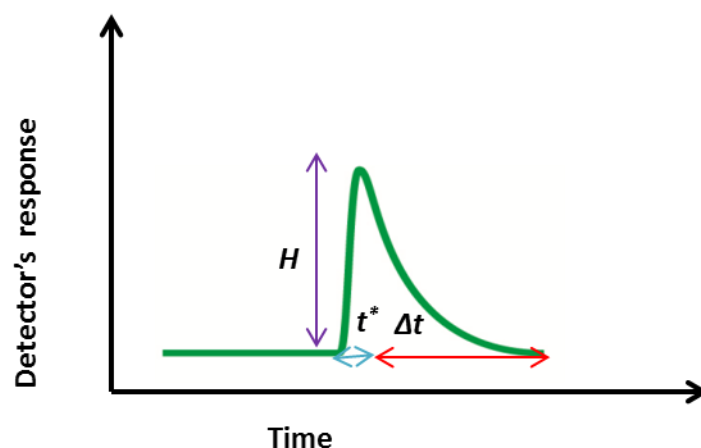


Figure 10. *The typical flow injection method curve.*

The parameters needed to describe the curve (Figure 10) are as follows:

- H is the peak height
- t^* is the difference between the residence time and travel time
- Δt is the time between the arrival of the sample's leading edge to the departure of its trailing edge

The most important parameters are the height of the peak, H , and return time, t^* . The peak height is related to concentrations of analytes and refers to the sensitivity of the FIA method. The return times determine the frequency with which we can inject samples. To describe the process quantitatively, the total dispersion coefficient, D_T , is used and it is given by the relation:

$$D_T = \frac{c_0}{c_{max}} = \frac{H_0}{H_{max}} \quad (2.5.1)$$

Where c_0 is the concentration of the injected sample, c_{max} is the maximum concentration of the sample, H_0 is the peak height (which corresponds to the concentration in the injection, c_0), and H_{max} is the maximum peak height (which corresponds to the concentration in the injection, c_{max}).^{67,68}

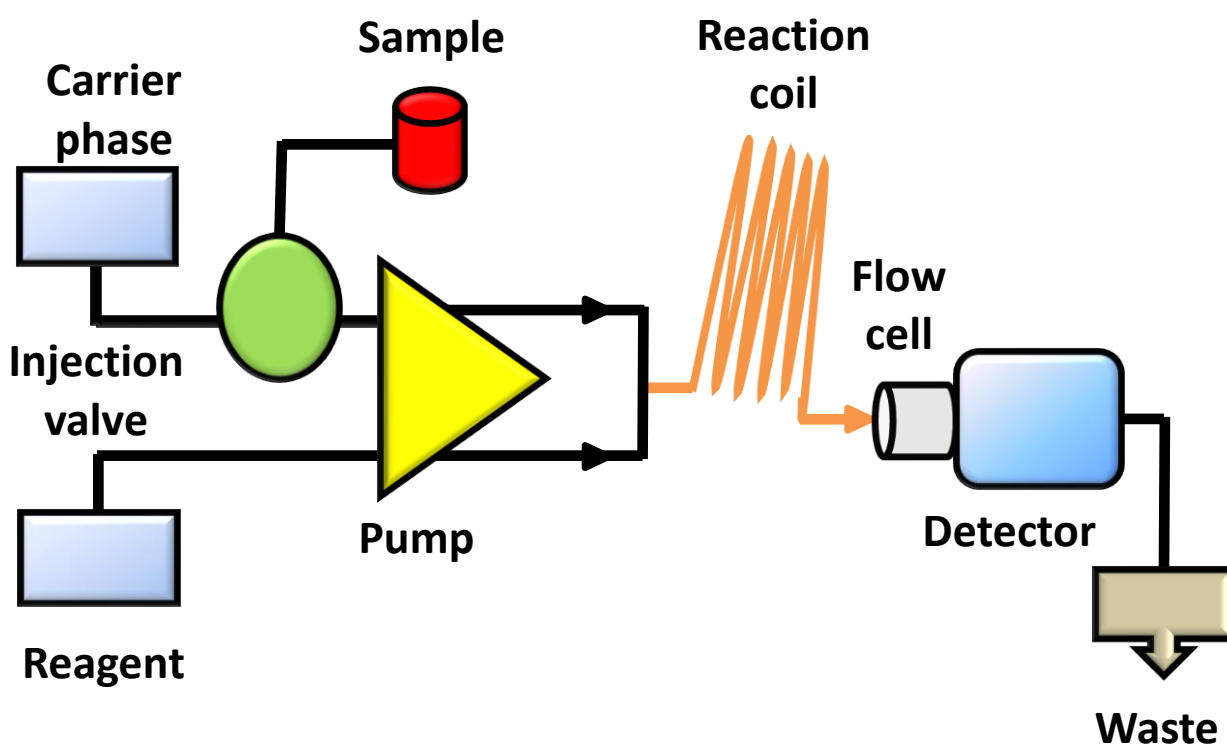


Figure 11. The schematics of the experimental setup in FIA. The simplest experimental setup consists of a peristaltic pump which is responsible for moving the carrier phase and an injection valve which is used for introducing the compounds. The setup is also equipped with the reaction coil (mixing chamber) and the detector which monitors the products.

2.5.1 Flow injection gradient method

The flow injection gradient technique can also be applied for determination of the association constant. In the experiment a known amount of the compound is introduced. The samples are injected precisely into the carrier phase. The concentration gradient is created by different devices, e.g. a mixing chamber. This gradient replaces the manual preparation of different concentrations of the samples. To obtain the profile of the concentration gradient, a detection during the flow is required (flow cell). In some systems a spectrometer with diode array system is used. However, this kind of detection is characterized by low sensitivity and high cost. In this case the problem can be solved by using an acousto-optic tunable system or changing the detector for e.g. an UV-Vis spectrometer.⁶⁹

In flow injection gradient analysis the determination of the association constant is based on the changes of the absorption for free and bound ligands. The absorption profile corresponds to the concentration profile of the compounds. First of all, to obtain the association constant it is necessary to create the concentration gradient of the ligand as a function of time. The gradient should be calibrated for compounds used in the experiments (for which the molar extinction coefficient is known). The maximum of the absorption is reached when the mixing is completed. Next, only the dilutions of the compounds are observed. These dilution profiles generate various concentration profiles with different dispersion coefficients. To calculate the association, constant plotting of the dispersion coefficient as a function of time is useful:

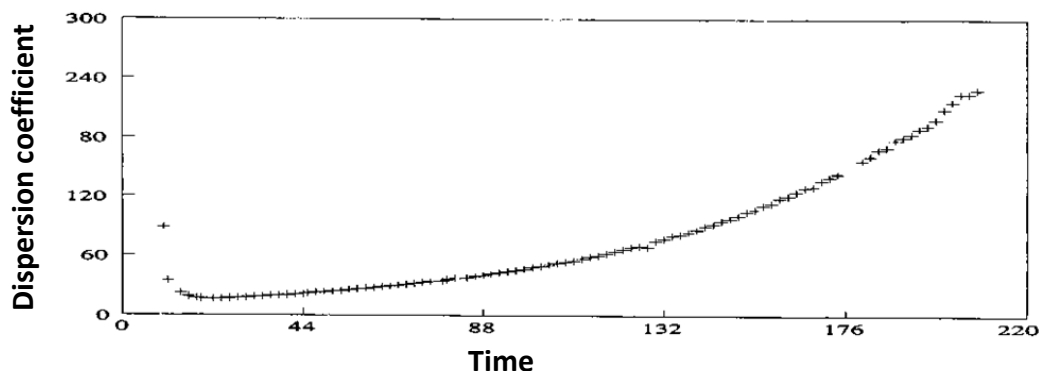


Figure 12. Dispersion coefficient as a function of time. Exemplary graph for a phenolphthalein solution in a carbonate buffer (pH=10.5 ; flow rate 3mL/min).

The dispersion coefficient, D_T , indicates the dilution of the analyte at a specific time:

$$D_T = \frac{[L]_0 \varepsilon}{A_{Time}} \quad (2.5.1)$$

Where $[L]_0$ is the concentration of stock solutions of the substrate molecule, ε is molar extinction coefficient, and A_{Time} is the absorbance measured as a function of time.

The dispersion coefficient as a function of time can be exchanged also for the dependence of the concentration on time. In this way we obtain a characteristic binding isotherm (based on the theoretical model). From the linear procedure including the creation of an isotherm and fitting the experimental data (to this linear binding isotherm) we are able to determine the value of the association constant and estimate the error (subsection 1.4).

However, the flow injection gradient method has some disadvantages, the most important one being calibrating the system before the measurements. Calibration can be provided only for a substance which is present in the system and for which the molar

extinction coefficient is well known. Of course the calibration curve can be later used for different substances, but still the calibration process is required before measurements. Moreover, there is an assumption in the calibration procedure that the dispersion coefficient as a function of time is independent of the type and concentration of the molecule used in the calibration curve. Additionally, problems with the adsorption of substances in the system appear very often.⁷⁰

In our **flow injection method** the experiments are conducted at a high flow rate (31 cm/s) in a long (>15m), thin (250 μ m) and coiled capillaries. The compound of interest (10 μ l) is injected into the carrier phase, which moves by the Poiseuille laminar flow. At the detection point we measure the concentration distribution of the analyte (i.e. by UV-Vis detector), as depicted in Figure 13.

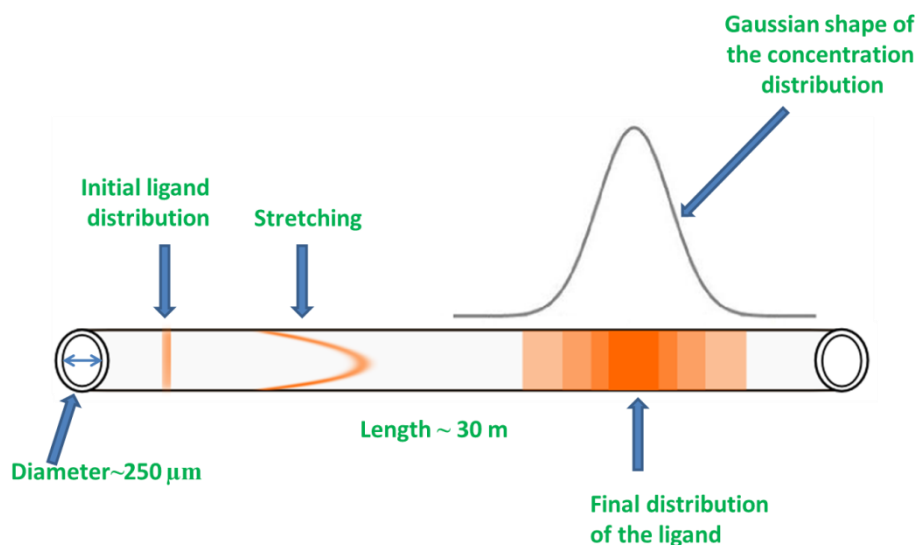


Figure 13. Dispersion in the capillary.

The width of the final profile of the analyte concentration is inversely proportional to the effective diffusion coefficient of the analyte. From the differences between the widths of the concentration distribution of free and bound ligand we determine the value of the association constant. In our method we do not have to calibrate the system before

every measurement. To sum up, the new method allows the researchers to determine the association constant in an easy, fast and more precise way.⁷¹

3. A new perspective of determination of the association constant by flow injection method: theoretical background

The purpose of this section is to provide the reader with the basic theoretical framework for interpreting the research presented in the experimental part of this work.

3.1 Dispersion in a straight capillary: Taylor dispersion method for determination of diffusion coefficient

Taylor dispersion theory was proposed by Taylor in 1953. It represents the process under ideal conditions in which the test substance is transported in an infinitely long and isothermal tube by laminar flow in the axial direction. At the injection point a solution of the substance is introduced. Due to the concentration gradient between the central part of the tube (capillary) and the walls, the solute diffuses in the radial direction. In appropriately selected conditions, the concentration of the diffusing substance is the Gaussian curve, and the flow of liquid reaches the average velocity u . This distribution is given by the following relation:⁷²

$$P(t) = \frac{1}{2\sqrt{\pi\sigma t}} \exp\left[-\frac{(L-ut)^2}{4\sigma t}\right] \quad (3.1.1)$$

Where σ is the dispersion coefficient, L is the distance between the injection and detection point, and t is time of measurement.

From the experiment, the dispersion of the substance by the UV-vis detector at wavelength λ is measured. According to the Taylor theory we calculate the molecular diffusion coefficient D from the measured dispersion coefficient σ . The dispersion coefficient, σ , is proportional to the square of the velocity, u , and inversely proportional to the effective molecular diffusion coefficient D_{eff} :⁷³⁻⁷⁵

$$\sigma = \frac{u^2 R^2}{48 D_{eff}} \quad (3.1.2)$$

Where R is the radius of the capillary.

3.2 Dispersion in a coiled capillary

Coiling of the capillary has a huge impact on analyte dispersion (the width of the peak).

In a coiled capillary, centrifugal force is generated due to the curved path of the flow.⁷⁶

In a straight capillary or for low flow rates (see Taylor theory) of carrier phase this force is negligible. The centrifugal force causes local generation of vortices, which additionally mix the analyte (Figure 14). It leads to narrowing of the analyte distribution along the capillary - several times in comparison to the concentration distribution at low flow rates or in the straight capillary. To determine the diffusion coefficient at high flow rates we used coiled capillaries, high flow rates (up to 31 cm/s) and the scaling equation:⁷⁵

$$D = -\frac{1}{48} \frac{u^2 R^2}{\sigma_c A \cdot \text{Lambert W} \left(-1, -\frac{1}{192} \frac{r \gamma e^{-\frac{B}{A}}}{R \rho \sigma_c A} \right)} \quad (3.2.1)$$

Where σ_c is the dispersion coefficient in a coiled capillary, ρ is the density of the carrier phase, γ is the viscosity of carrier phase, R is the internal capillary radius, and r is the external radius of curvature of the coiled capillary; $A = 0.87 \pm 0.02$ and $B = -3.8 \pm 0.2$ are fitted parameters. Formula 3.2.1 can be simplified by replacing the function LambertW $(-1, x)$ with its asymptotic expansion:

$$\text{Lambert W}(-1, x) \approx W(x) = L_1 - L_2 + \frac{L_2}{L_1} + \frac{L_2(-2+L_2)}{2L_1^2} \quad (3.2.2)$$

Where $L_1 = \ln(-x)$ and $L_2 = \ln(-\ln(-x))$.

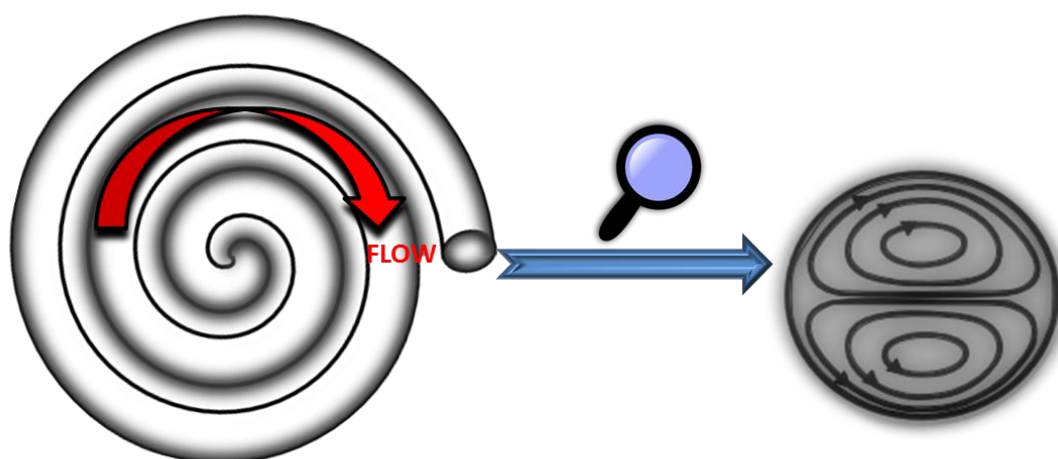


Figure 14. Schematic representation of vortices appearing in a coiled capillary at high flow rates.

Equation 3.2.1 works well for different substances, velocities, volumes of injection, radii of the capillary and radii of coiling of the capillary. Additionally, the equation leads to shortening of measurement time to minutes.⁷⁵

3.3 Straight capillary vs coiled capillary

Straight capillary. The estimation of the width of the peak, given by relation 3.1.2 is possible only in a long capillary and at low flow rates of the carrier phase. The problem is the experiment length. A single experiment performed at low flow rates takes about 50 minutes. For longer capillaries this time is even longer. Additionally, the determination of the diffusion coefficients at low flow rates has an error (about 30%), for macromolecules (i. e. proteins).⁷⁷ The solution describing the dispersion of the analyte at high flow rates of the carrier phase is proposed by Lewandrowska, A.; Majcher, A.; Ochab-Marcinek, A.; Tabaka, M.; Holyst, R. *Anal. Chem.* **2013**, 85, 4051–4056.

Coiled capillary. At high flow rates the vortices are mixing the analyte across the capillary and they reduce the width of the concentration distribution several times in comparison to the results obtained at low flow rates (or in a straight capillary). Therefore determination of the diffusion coefficients at high flow rates eliminates the error (about 30%) present for macromolecules (i.e. proteins) at low flow rates. The reason of this divergence is the time of flow. Such time has to be much longer than the time needed for a protein to diffuse across the capillary. In a capillary ($L=30$ m is the length of the capillary) with internal radius $R=250$ μm and at the velocity $u = 0.9$ $\text{cm}\cdot\text{s}^{-1}$ we have not very good accuracy. To obtain error lower than 5% a very long capillary (about 100 m) should be used (according to the condition $L/u \gg R^2/D$). Using such a long capillary leads to wasting the reagents and lengthening of the measurement time. Application of the empirical equation described in Analytical Chemistry results in an increase of precision and a decrease in uncertainty of the measurements. In summary, to obtain the correct value of the association constant (based on the values of the diffusion

coefficients) we should use the proper length of the capillary (or the capillary should be thinner). The aim of my work is to apply high flow rates and scaling equation (described by Lewandrowska, A.; Majcher, A.; Ochab-Marcinek, A.; Tabaka, M.; Holyst, R. *Anal. Chem.* **2013**, 85, 4051–4056) for determination of diffusion coefficients needed for determination of the K_a .

3.4 Determination of the association constant based on the diffusion coefficient using flow injection method

To determine the association constant (based on the values of diffusion coefficients, D) three separate experiments are needed. First, diffusion coefficient of the ligand, D_L , is determined using a buffer solution as a carrier phase. Next we determine a diffusion coefficient of the macromolecule, D_M (buffer as the carrier phase). Finally, we fill the whole capillary with a solution of the macromolecule having the same concentration as the sample injection, and we determine an effective diffusion coefficient, D_{eff} . In all the experiments concentration of the ligand changes during the flow (is diluted even hundreds times during the flow). Determination of diffusion coefficients of the compounds is based on the differences in the widths of concentration distributions (dispersion coefficient, σ), as depicted in Figure 15.

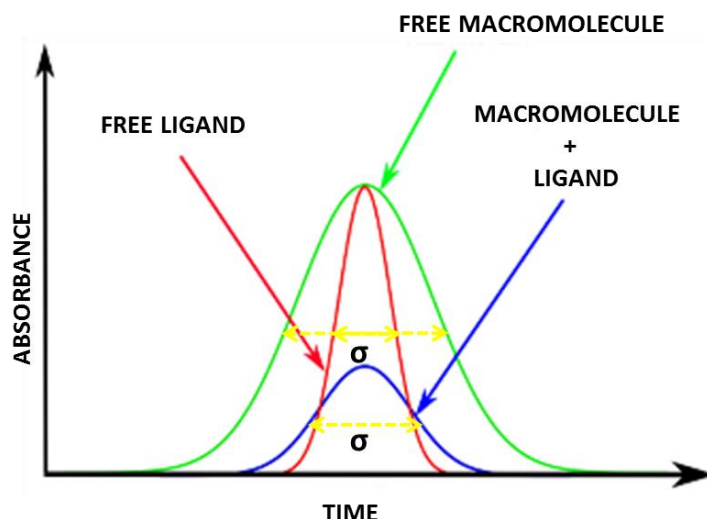


Figure 15. The dispersion coefficient, σ of the free ligand, free macromolecule and ligand-macromolecule complex. The dispersion coefficient, σ , is defined as the width of the peak at half of its height.⁷¹

The determination of the association constant can be shortly described as follows: we inject a ligand with a macromolecule into the capillary filled with the solution of the macromolecule (the concentration of the macromolecule solution is the same as in the injected sample). They flow together and bind to form a complex. The interaction between the ligand and the macromolecule causes a decrease of the effective diffusion coefficient, D_{eff} , because the ligand diffuses temporarily together with the macromolecule, thus slower than the free ligand. A schematic representation of the interaction between the ligand and the macromolecule is presented in Figure 16.

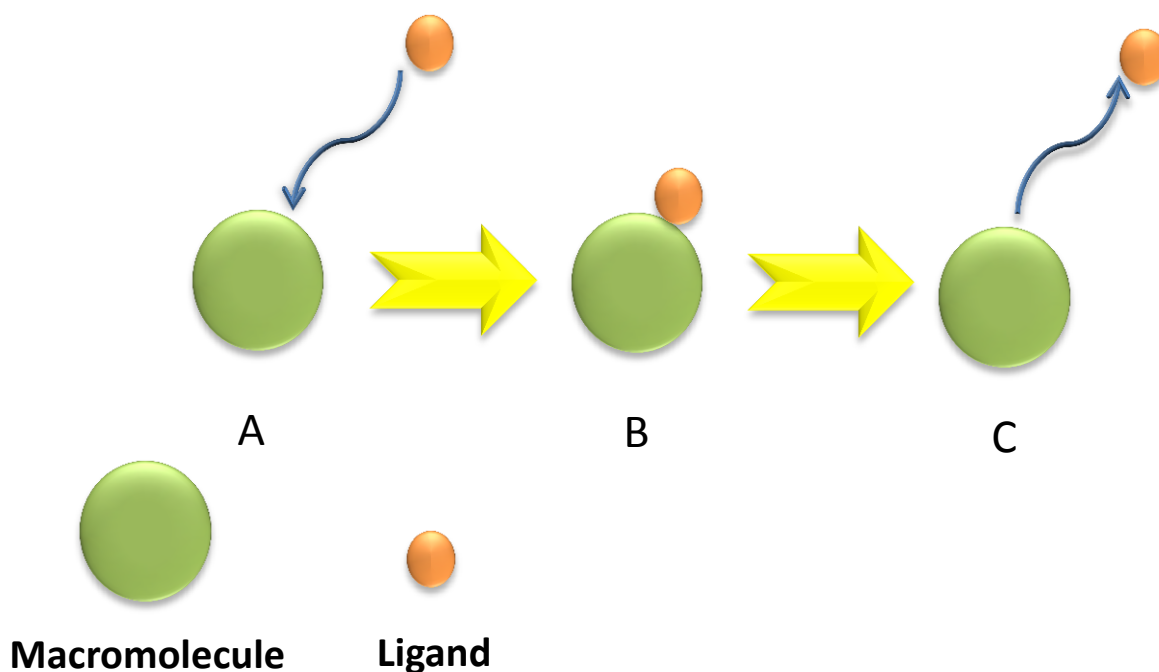


Figure 16. (A) Free ligand and free macromolecule, (B) binding of the ligand to the macromolecule, (C) unbinding of the ligand from the macromolecule.

A ligand and a macromolecule spend some time separately (Figure 16 A and C) and some time as a complex (Figure 16 B). As a consequence the following relation holds:

$$D_{eff} = \frac{D_L t_L + D_{LM} t_{LM}}{t_L + t_{LM}} \quad (3.4.1)$$

Where t_L is time spent by the ligand in the free state, t_{LM} is a time spent in a bound form, D_{eff} is a diffusion coefficient [$\frac{\text{cm}^2}{\text{s}}$] of the ligand in the presence of the macromolecule, D_L is a diffusion coefficient [$\frac{\text{cm}^2}{\text{s}}$] of the free ligand, and D_{LM} [$\frac{\text{cm}^2}{\text{s}}$] is diffusion coefficient of the complex.

The ratio of $\frac{t_{LM}}{t_L}$ is related to the equilibrium constant for the complex formation:

$$K_a c_M = \frac{c_{LM}}{c_L} = \frac{t_{LM}}{t_L} \quad (3.4.2)$$

where K_a is the association constant [M^{-1}], c_M is macromolecule concentration, much higher than the ligand concentration (the capillary is filled with a solution of the macromolecule), c_L is the concentration of the ligand, and c_{LM} is the concentration of the complex.

Combining Eq (3.4.1) and Eq (3.4.2) we obtain the following dependence between effective diffusion coefficient and the equilibrium constant:

$$D_{eff} = \frac{D_L + D_{LM} K_a c_M}{1 + K_a c_M} \quad (3.4.3)$$

The diffusion coefficient of the ligand is much larger ($D_L \gg D_M$) than the diffusion coefficient of the macromolecule. Therefore, we can approximate the diffusion coefficient of the complex by the diffusion coefficient of the macromolecule. Thus, the effective diffusion coefficient is equal to:

$$D_{eff} = \frac{D_L + D_M K_a c_M}{1 + K_a c_M} \quad (3.4.4)$$

The equation (3.4.4) can be transformed to the following form:^{75,77}

$$K_a = \frac{(D^{eff} - D_L)}{(D_M - D^{eff}) c_M} \quad (3.4.5)$$

which is directly applicable to our measurements presented in the next section.

4. Experimental part


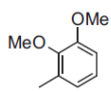
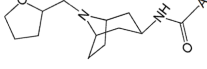
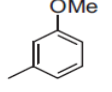

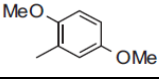
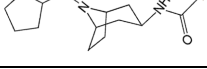
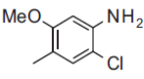
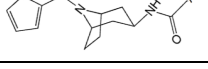
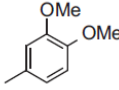
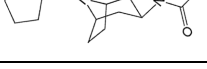
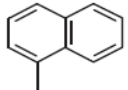

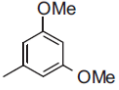
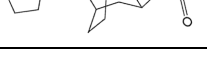
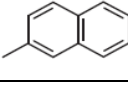

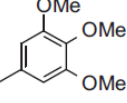

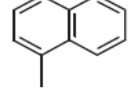

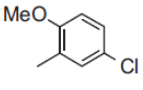
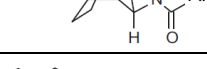
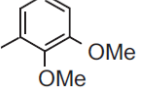

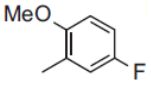
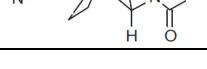
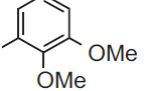
4.1 Chemicals

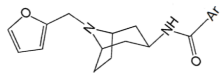
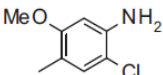
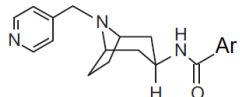
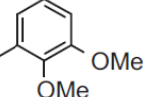
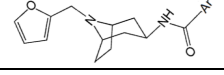
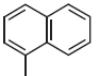
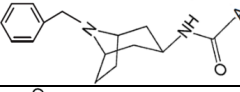
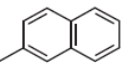
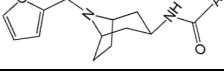
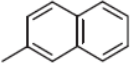
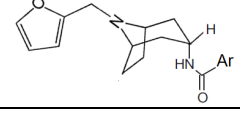
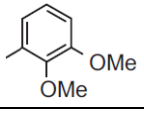
Drug/BSA systems

Warfarin, sulindac, diflunisal, fenbufen, etodolac, cefaclor / Bovine serum albumin (BSA) were purchased from Sigma-Aldrich (Germany).

Potential drug/BSA systems

The 3 β - and 3 α -aminotropane derivatives (compounds 1–20) were synthesized at the Department of Drug Technology and Pharmaceutical Biotechnology at the Medical University of Warsaw.

No of compound	Compound	Substituent (Ar)	No of compound	Compound	Substituent (Ar)
1.			11.		
2.			12.		
3.			13.		
4.			14.		
5.			15.		
6.			16.		
7.			17.		

8.			18.		
9.			19.		
10.			20.		

Surfactant/dye systems

Hexadecyltrimethylammonium Chloride (CTAC), (TCI Europe N.V., Belgium);
Sodium dodecyl sulfate (SDS), (Carl Roth, Germany); Atto 488 Protein Labeling Kit,
Rhodamine 110 Chloride (Sigma-Aldrich, Germany).

Protein/DNA system

Oligonucleotides (FutureSynthesis Sp. z o. o., Poland); Interferon regulatory factor
9 (IRF9), (EMBL-EBI, UK).

Other substances used in the experiments:

Alpha-tris-(hydroxymethyl)-methylamine (Tris), (Carl Roth, Germany), Ortho-
phosphoric acid (H₃PO₄), (POCH, Poland).

All the above compounds were used with no further purification or modification.

4.2 Equipment

The experiments are carried out using an apparatus from Shimadzu Corporation (Kyoto, Japan). The flow injection equipment consists of the pump (LC-20 AD), degasser unit (DGU-20 A_{3R}), autosampler (SIL-20AHT), capillary (Applied Research Europe GmbH, Germany), thermostat (CTO- 20AC) and two detectors: UV-Vis (SPD-20A) and fluorescence detector (RF-20Axs). Additionally, heating controller (ESM-3711-H bought from Laboplay, Poland) is used for keeping proper temperature of carrier phase. The pump with pistons lets manipulate the volume of flow rate ranging from 0,0001 to 5 ml/min. The flow rate of the solutions is generated by applying pressure in the range of 1,0-40 MPa. Carrier phase flows through long (30m), thin (0,25mm), polymeric (PPEK) capillary. The temperature (25°C) of the carrier phase is stabilized by a heating controller. A degasser unit removes bubbles of air from the carrier phase. An autosampler is used for injection of the analyzed substances. As much as 100 samples prepared in an appropriate way are inserted into the autosampler. The volume of injection ranges from 0,1 up to 100 µL. The capillary is thermostated in an oven, which can maintain constant temperature in the range of 4-85 °C. At the end of the capillary a UV-Vis detector is situated equipped with a deuterium lamp (working in the range 190-370 nm) and a tungsten lamp (working in the range of 371-900 nm). A second detector is a spectrofluorometric one, also equipped with a low-pressure mercury lamp (to check wavelength accuracy) and a xenon lamp (working in the range of 200-750 nm). All equipment is connected to the computer software (LCsolution 1.25), allowing the researchers to analyze results in detail.



Figure 17. *The experimental setup: 1- heating controller; 2- pump; 3- autosampler; 4- degasser unit; 5- thermostat; 6- capillary; 7- UV-Vis detector; 8- fluorescence detector; 9- computer.*

4.3 Determination of the capillary radius

As commercially available capillaries (made of polyether ether ketone, PEEK) are not uniform, it is necessary to determine a capillary radius experimentally. Estimation of the radius was conducted using 18 mM TRIS solution as a carrier phase, adjusted to pH = 7.4 with H₃PO₄, as well as a dry, thin (0.25 mm) and 30 meter long capillary. The time of filling the capillary by the TRIS solution was measured (the density of the carrier phase was known). We obtained the effective radius of $r = 0.13$ mm. Due to

excessive length of the capillary it had to be coiled to fit into the oven. The radius of curvature of the capillary was 8 cm.



Figure 18. A PEEK capillary inside the oven.

5. Application of the theory for determination of the association constant by flow injection method

5.1 Drug-protein interactions: a test of the method

This method was tested and verified for a number of complexes of selected drugs (cefaclor, etodolac, sulindac) with albumin (BSA). The concentrations were as follows: cefaclor $C_L = 8.16 \times 10^{-4}$ M, etodolac $C_L = 1.04 \times 10^{-3}$ M and sulindac $C_L = 1.68 \times 10^{-4}$ M. Concentration of BSA (macromolecule) was $C_M = 9.03 \times 10^{-5}$ M. First, a 18 mM tris solution at pH 7.4 was used. Then, a sample of the ligand (drug) was injected into this solution. In the last step we filled the whole capillary with

a solution of BSA and injected a ligand-macromolecule sample (concentration of the macromolecule in the sample was the same as in the carrier phase). Due to the changes in the width of the concentration distribution for free and bound ligand (drug) we determined the association constant for ligand-macromolecule complex formation.

Table 1. Comparison of association constants of selected drugs with BSA determined by flow injection method at high flow rates of a carrier phase (equation 3.4.5) and literature values of association constants for these biochemical systems. The accuracy of the measurements of the association constants is included in the table.

Drug + BSA	K_a [M^{-1}] Measurements at high flow rates	K_a [M^{-1}] (Literature data)	Accuracy [%]
cefaclor	$(4.45 \pm 0.57) \times 10^3$	3.30×10^3	34.8
etodolac	$(1.00 \pm 0.15) \times 10^5$	1.30×10^5	23.1
sulindac	$(1.03 \pm 0.03) \times 10^5$	1.10×10^5	6.36

*Uncertainties in the brackets are standard deviations of arithmetic mean multiplied by critical value in a t-student distribution $t_{n,\alpha}$.

§The values of diffusion coefficient of free ligands needed for determination of the association constant were collected from the PhD thesis of Anna Zagożdżon titled "Development of the Taylor dispersion method for diffusion coefficient measurements",⁷⁸

We determined the association constants for known drugs with BSA. We conducted experiments at a high flow rate (31 cm/s) of the carrier phase in a coiled capillary. We compared our results with the literature data. The data we obtained was in very good agreement with data collected from the literature.

5.2 Comparison of association constants obtained at high and low flow rates of a carrier phase

We conducted experiments at high (31 cm/s) and low flow rate (1.5 cm/s) of the carrier phase. The results are presented for cefaclor/BSA, etodolac/BSA, and sulindac/BSA systems. Concentration of the compounds was the same as in previous experiments. The values of association constant obtained at high flow rates differ significantly from the data obtained at low flow rates of the carrier phase. Only the data for high flow rates give reliable results for K_a (subsection 3.3).

Table 2. Comparison of association constants of some drugs determined by flow injection method at high and low flow rates (equation 3.4.5) and values of association constants of these compounds taken from the literature.

Drug + BSA	K_a [M^{-1}] Measurements at high flow rates	K_a [M^{-1}] (Measurements at low flow rates)	K_a [M^{-1}] (Literature data)
cefaclor	4.45×10^3	$(8.71 \times 10^3 \pm 0.06)$	3.30×10^3
etodolac	1.00×10^5	$(7.82 \times 10^4 \pm 0.02)$	1.30×10^5
sulindac	1.03×10^5	$(7.44 \times 10^5 \pm 0.03)$	1.10×10^5

*Uncertainties in the brackets are standard deviations of arithmetic mean multiplied by critical value in a t-student distribution $t_{n,\alpha}$.


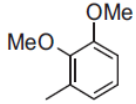

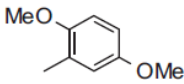
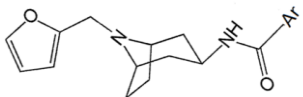
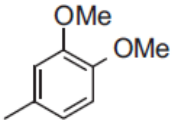
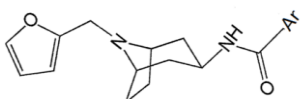
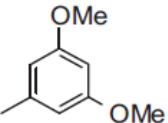

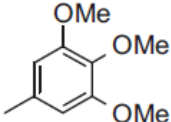
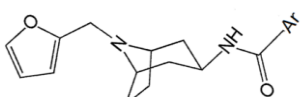
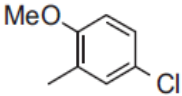
§The values of diffusion coefficient of free ligands needed for determination of the association constant were collected from PhD thesis of Anna Zagożdżon titled "Development of the Taylor dispersion method for diffusion coefficient measurements"

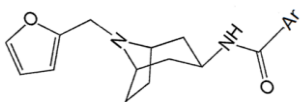
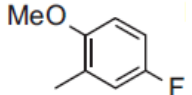

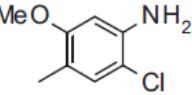
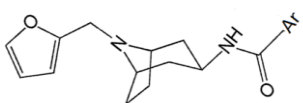
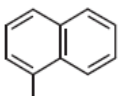
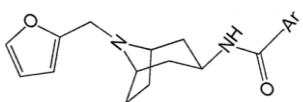
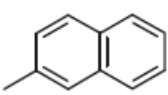
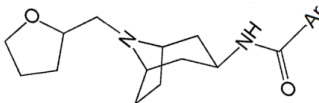
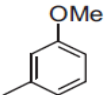
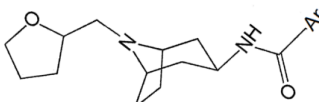
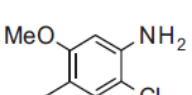
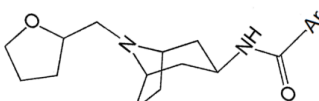
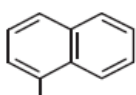
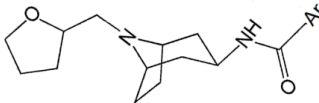
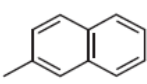
We also conducted experiments at low flow rates (Taylor's equation was used for calculation of diffusion coefficient) of a carrier phase. We compared our results with data obtained at high flow rates and with the literature. The values of association constant differ significantly. The reason lies in the time of the flow, $t=L/u$. During the flow the analyte diffuses many times across the capillary i.e. $L/u \gg R^2/D$ (L is the length of capillary, u is the velocity, R is the radius of the capillary, D is the diffusion coefficient of the compound). In the conditions of the experiment ($L=30$ m, $R=250$ μm , velocity $u = 0.9$ cm s^{-1}) the error of determination of a diffusion coefficient is too large - for example, for proteins it is about 15-30%. This systematic error grows along with molecular mass and flow velocity. To summarize, the time of the flow needs to be much longer than the time needed for a protein to diffuse across a capillary. The criterion $L/u \gg R^2/D$ is fulfilled for very long capillaries (>100 m) or very thin ones ($\ll 250$ μm). Nevertheless, the best solution is to use high flow rates of the carrier phase. High velocities cause appearance of vortices which mix the analyte, allowing to fulfill the condition $L/u \gg R^2/D$ (the empirical equation described in Analytical Chemistry is required).


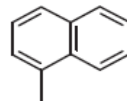
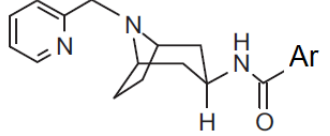
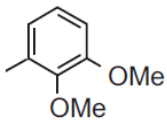
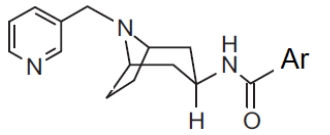
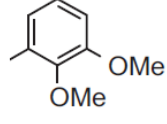
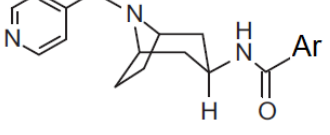
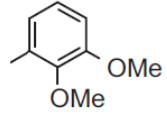

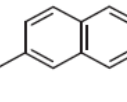
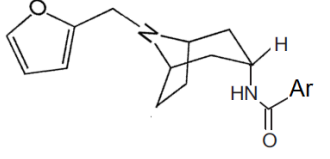
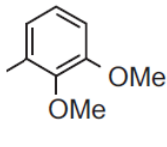
5.3 Application of the method to complexes of BSA with 3 β - and 3 α -aminotropane derivatives

The experiments were conducted in the same conditions and according to the same procedure as described above. The concentrations of the solutions of the macromolecule (BSA) ranged from $C_M = 4.5 \times 10^{-3}$ M to $C_M = 9.5 \times 10^{-5}$. The concentrations of 3 β - and 3 α -aminotropane derivatives (potential antipsychotic drugs) ranged from $C_L = 8.59 \times 10^{-4}$ M to $C_L = 6.49 \times 10^{-4}$ M.

Table 3. The association constants of 3 β - and 3 α - aminotropane derivatives (compounds 1-20) with BSA - experimental values (equation 3.4.5). The standard deviations of the measurements of the association constants are included in the table.

No of compound	Compound	Substituent (Ar)	K_a [M^{-1}] $\times 10^{-2}$	$SD_{\bar{x}t}$ (n=3) $\times 10^{-2}$	$RSD_{\bar{x}t}$ %
1.			24	1.9	7.8
2.			4.2	0.18	4.2
3.			6.1	0.90	14.9
4.			No detectable interaction	-	-
5.			43	2.9	6.7
6.			No detectable interaction	-	-

7.			9.73	0.4	4.1
8.			5.76	0.65	11.3
9.			4.19	0.90	21.5
10.			28	5.1	15.2
11.			60	0.72	1.2
12.			2.19	0.18	8.2
13.			14	0.71	5.0
14.			41.8	1.1	2.6

15.			20.1	1.6	7.8
16.			27.9	1.3	4.6
17.			43.5	0.96	2.2
18.			40	2.6	6.5
19.			No detectable interaction	-	-
20.			5.80	0.72	12.5

[§]The values of diffusion coefficient of free ligands need for determination of the association constant were collected from the PhD thesis of Anna Zagożdżon titled "Development of the Taylor dispersion method for diffusion coefficient measurements".

All compounds were synthesized by the group headed by Professor F. Herold from the Department of Drug Technology and Pharmaceutical Biotechnology at the Medical University of Warsaw.

We determined the association constant of 3 β - and 3 α -aminotropane ligands of 5-HT_{1A}, 5-HT_{2A} and D₂ receptors with BSA. These derivatives have different size,

substituents and conformation. The 3 β - and 3 α -aminotropane ligands exhibit potential antipsychotic activity. The association constants range from $K_a = 10^2$ to $K_a = 10^3 \text{ M}^{-1}$. The results show that these potential drugs bind weakly to the bovine serum albumin and a lower dose of these drugs is able to exert the pharmacological effect.

5.4 Technical limitations of the method: range of concentrations and association constants

In the experiments we used sulindac as a ligand. The initial concentration of this drug was $C_L = 1.68 \times 10^{-4} \text{ M}$. The final concentration was $C_{L(\text{final})} = 2.13 \times 10^{-6} \text{ M}$. This concentration of the ligand was estimated based on the following relation:

$$C_{L(\text{final})} = C_{L(\text{injection})} \frac{L_{\text{injection}}}{L_{\text{final}}} \quad (5.4.1)$$

where $C_{L(\text{final})}$ was the ligand concentration at the end of the capillary, $C_{L(\text{injection})}$ was the ligand concentration in the sample, $L_{\text{injection}}$ was the injection width, and L_{final} was the final concentration distribution length.

Equilibrium concentrations of the reagents were calculated from the equation:

$$K_a = \frac{C_{LM}^{eq}}{(C_{L(\text{final})} - C_{LM}^{eq})(C_M^0 - C_{LM}^{eq})} \quad (5.4.2)$$

where K_a is the association constant at equilibrium; C_{LM}^{eq} is a concentration of the complex at equilibrium; $C_{L(\text{final})}$ is the overall concentration of the ligand at the capillary end; C_M^0 is an overall concentration of the macromolecule ($C_M \gg C_{LM}^{eq}$).

We tested concentrations of the macromolecule in carrier phase ranging from $C_M = 3.01 \times 10^{-7} \text{ M}$ to $C_M = 9.03 \times 10^{-5} \text{ M}$.

Table 4. *Equilibrium concentrations of the free ligand, $C_{L(\text{equilibrium})}$ the free protein, C_M (equilibrium) and the complex, C_{LM} (equilibrium) at different concentrations of the protein (BSA). The whole capillary was filled by a macromolecule solution.*

Concentration of BSA in the carrier phase	9.03×10^{-5}	1.81×10^{-5}	3.01×10^{-6}	1.5×10^{-6}	9.03×10^{-7}	3.01×10^{-7}
$C_{L(\text{equilibrium})} [\text{M}]$	2.16×10^{-7}	7.96×10^{-7}	1.69×10^{-6}	1.89×10^{-6}	1.98×10^{-6}	2.08×10^{-6}
$C_{M(\text{equilibrium})} [\text{M}]$	8.84×10^{-5}	1.68×10^{-5}	2.57×10^{-6}	1.26×10^{-6}	7.54×10^{-7}	2.49×10^{-7}
$C_{LM(\text{equilibrium})} [\text{M}]$	1.91×10^{-6}	1.33×10^{-6}	4.36×10^{-7}	2.39×10^{-7}	1.49×10^{-7}	5.18×10^{-8}

The association constant depends to certain extent on protein concentration in the carrier phase. This dependence is presented in Table 5. It is the systematic error for small concentrations.

Table 5. *Dependence of the association constant of sulindac-BSA at different concentrations of the protein. Final concentration of sulindac was the same in each experiment ($C_{L(\text{final})} = 2.13 \times 10^{-6} \text{ M}$).*

$C_{\text{BSA}} [\text{M}]$	9.03×10^{-5}	1.81×10^{-5}	3.01×10^{-6}	1.5×10^{-6}	9.03×10^{-7}	3.01×10^{-7}
$K_a [\text{M}^{-1}]$	1.03×10^5	1.09×10^5	1.20×10^5	1.34×10^5	No detectable interaction	No detectable interaction

In the determination of the association constant the error was about 30%. The error was related to a formation of fewer and fewer number of complexes for lower and lower concentrations of BSA. A fewer number of complexes indicates inaccuracies in an estimation of widths of concentration profiles. Below the concentration of $C_M = 1.5 \times 10^{-6}$ M we did not observe any differences between the width of the concentration distribution of the sulindac-BSA system and the width of concentration distribution of sulindac in a buffer solution. The minimum concentration of a protein solution (enough to observe changes in concentration profiles) depends on the concentration of the injected ligand and the value of the association constant.

To detect differences between concentration distribution for the free ligand, the free macromolecule and the complex, the following conditions (a and b) need to be fulfilled:

$$\text{a) } 0.1 C_{L(\text{injection})} \frac{L_{\text{injection}}}{L_{\text{final}}} < C_{LM}^{\text{eq}} < 0.9 C_{L(\text{injection})} \frac{L_{\text{injection}}}{L_{\text{final}}} \quad (5.4.3)$$

Where $C_{L(\text{injection})}$ is the ligand concentration in an injected sample, $L_{\text{injection}}$ is the injection width, L_{final} is the final length of the concentration distribution, and C_{LM}^{eq} is the concentration of the complex at equilibrium.

The condition (a) is related to the final concentration of the complex, C_{LM}^{eq} , and indicates when it is possible to observe interactions. If C_{LM}^{eq} of the complex is higher than 90% of $C_{L(\text{injection})} \frac{L_{\text{injection}}}{L_{\text{final}}}$ in our experiments only the signal from the complex is observed. If C_{LM}^{eq} of the complex is lower than 10% of $C_{L(\text{injection})} \frac{L_{\text{injection}}}{L_{\text{final}}}$, only the peak from the ligand is observed.

$$\text{b) } \frac{D_M - D_L}{XD_M} \gg Kc_M \gg \frac{XD_L}{D_M - D_L} \quad (5.4.4)$$

Where D_M is the diffusion coefficient of the protein, D_L is the diffusion coefficient of the ligand, and X is precision of determination of diffusion coefficient.

The condition (b) is related to the precision of determination of the diffusion coefficient, D_M . The diffusion coefficient of the macromolecule (in this case protein) is about 10 times smaller than the diffusion coefficient of the ligand. The precision, X , of determination of the diffusion coefficient is usually to a few percent (for example it is 3% for the sulindac-BSA system). Therefore Eq. (5.4.4) was written as follows:

$$300 \gg Kc_p \gg 0.03 \quad (5.4.5)$$

The determination of the association constant is possible when the differences between the dispersion coefficient (the widths of peaks) of the free ligand and the ligand which interacts with the proteins are measurable. We show a case when the differences between the widths of the concentration distribution are indiscernible (the condition (b) is not fulfilled), as depicted in Figure 19.

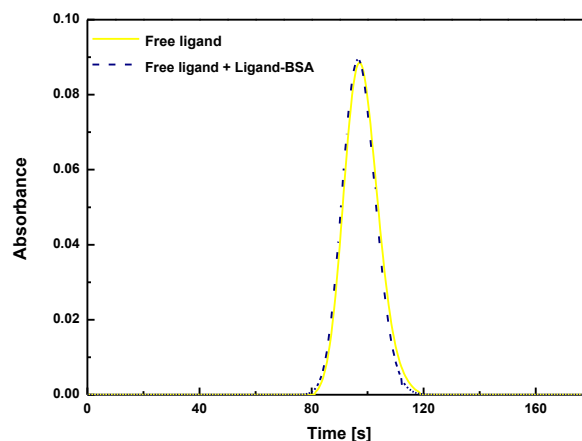


Figure 19. *The widths of the concentration distribution of the free ligand and ligand which interact with the protein. The differences between the widths of the concentration distribution are too small to determine association constant. The results are shown for free sulindac and sulindac-BSA system.*

In our considerations we proved that the UV-Vis detection was possible if conditions (a) and (b) were fulfilled (Equations 5.4.3 and 5.4.4). To determine an association constant, the widths of concentration profile for a free ligand and the ligand in a presence of the macromolecule need to be measurable. Additionally, we showed that in our experiments the limitation was the concentration of the ligand, which in turn was limited by the sensitivity of the detector and ligand's solubility in a buffer solution.

6. A new perspective of determination of the association constant by flow injection method

Filling the whole capillary with a solution of the macromolecule is a waste of expensive compounds. Additionally, for some macromolecules large amounts are not available. That is why we decided to modify our experiments. The purpose of this work was to decrease the amount of macromolecule used in the experiments (in the previous version

of the experiment the capillary was filled with the macromolecule solution where the volume of the capillary was 1.6 ml and the concentration of the protein was 10^{-6} - 10^{-5} M). The new concept of conducting experiments was as follows: we inject a ligand with the macromolecule (total volume of 10 μ l) into the capillary without filling it with macromolecule solution. We let them flow together and bind to form complexes. The experiment is outlined in Fig. 20.

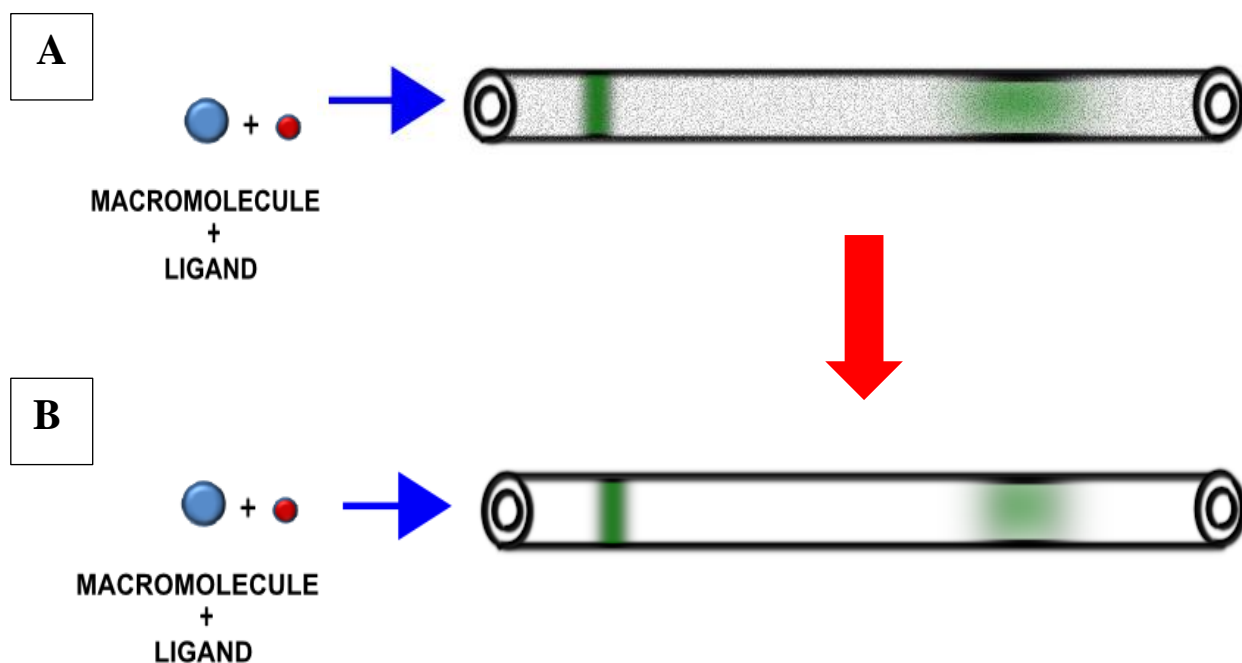


Figure 20. Two types of experiments. (A) A ligand–macromolecule solution is injected into carrier phase (a solution of the macromolecule). (B) A ligand–macromolecule sample is injected into buffer solution. A complex is formed during the flow.

6.1 Reduction of the amount of reagents: experimental challenges

6.1.1 Overlapping of peaks

In the previous versions of the experiment, the capillary was filled with a solution of the macromolecule (in these experiments we reset the signal from BSA). In our new method of conducting experiments we inject a ligand with the macromolecule as a single injection into the capillary filled with a buffer solution. In these experiments we observed an overlapping of peaks because a lot of substances (especially drugs) have an absorption spectrum at a wavelength similar to BSA. It leads to a non-symmetrical shape of the peak, as depicted in Figure 21.

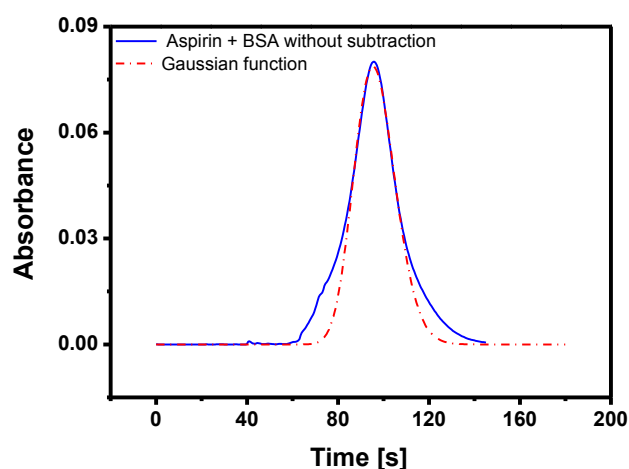


Figure 21. A comparison of the mixture of the drug with bovine serum albumin (single injection experiment) with the Gaussian function.

The absorbance is an additive quantity. We subtracted the absorbance of BSA from the absorbance obtained for the mixture. The results were highly satisfactory, as depicted in the figure below.

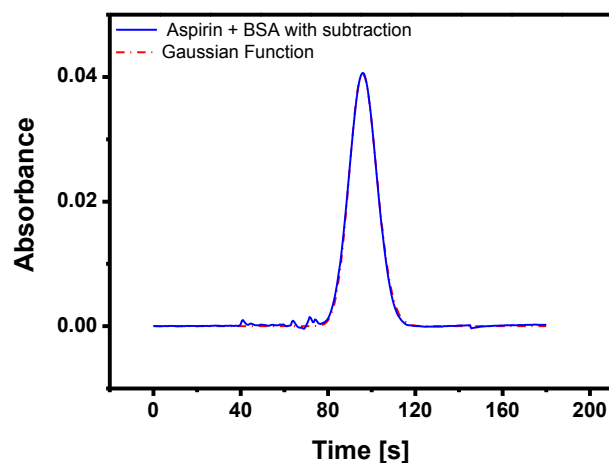


Figure 22. *A comparison of the mixture of drug with bovine serum albumin in single injection with the Gaussian function (after subtraction of the absorbance coming from bovine serum albumin). The concentration of macromolecule was the same as the concentration of the protein in the injection.*

6.1.2 Effective diffusion coefficient in a single injection experiment

The difference between the diffusion coefficient of the free ligand and the diffusion coefficient of the bound ligand is sufficient to determine the value of the association constant. Therefore, a very important part of the experiment is to check this difference and compare it to the effective diffusion coefficient obtained as a result of the interactions with the macromolecule during the flow.

Table 6. *The diffusion coefficient of free drugs and the effective diffusion coefficient of the drugs which interact with bovine serum albumin.*

Studied system	Diffusion coefficient of the free ligand [cm²/s]	Effective diffusion coefficient of the ligand [cm²/s]
Warfarin-BSA	$(4.83 \times 10^{-6} \pm 0.02)$	$(1.25 \times 10^{-6} \pm 0.01)$
Sulindac-BSA	$(3.95 \times 10^{-6} \pm 0.01)$	$(2.19 \times 10^{-6} \pm 0.02)$
Aspirin-BSA	$(6.79 \times 10^{-6} \pm 0.02)$	$(3.22 \times 10^{-6} \pm 0.01)$
Fenbufen-BSA	$(4.79 \times 10^{-6} \pm 0.02)$	$(8.33 \times 10^{-7} \pm 0.02)$

*Uncertainties in the brackets are standard deviations of arithmetic mean multiplied by critical value in a t-student distribution $t_{n,\alpha}$.

These differences between the diffusion coefficient of the free ligand and the effective diffusion coefficient of the ligand are significant. This means that determination of the association constant from them is possible.

6.1.3 Changes of macromolecule concentration at different flow rates

In previous versions of the experiment the concentration of the macromolecule was constant. Presently, the concentration of the macromolecule changes during the flow.

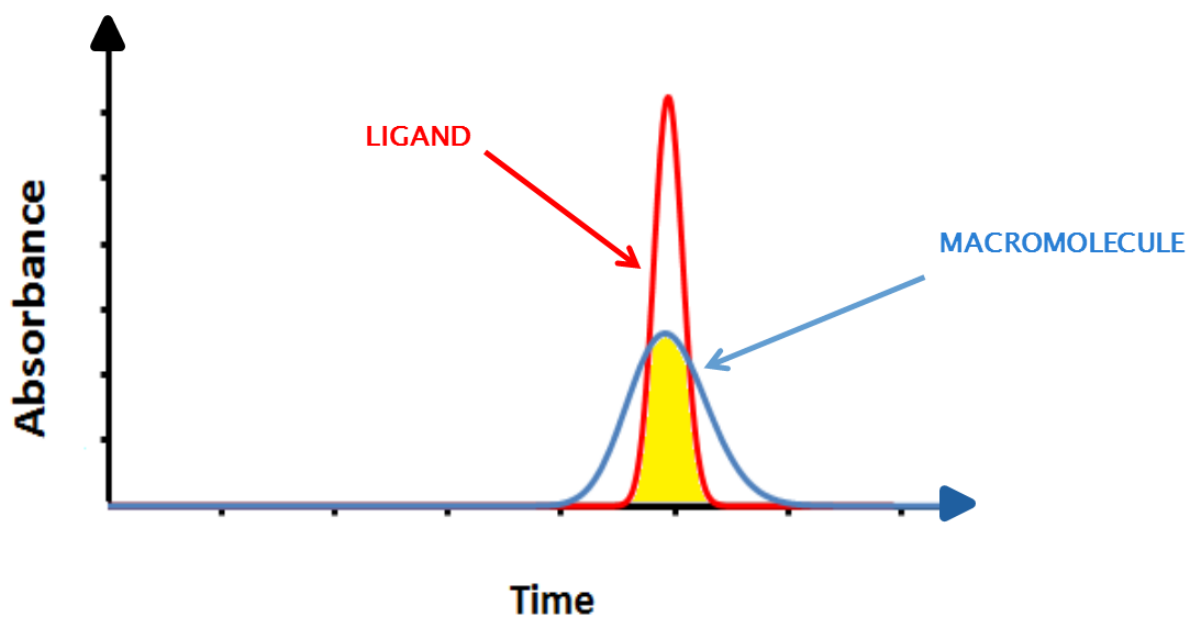


Figure 23. A schematic representation of the concentration changes for a ligand and the macromolecule during the flow. Yellow color indicates the concentration of the macromolecule which is available for the ligand.

In a single injection experiment we suspect that for different flow rates, F of a carrier phase concentration of macromolecule available for the ligand should be different for each flow rate. Therefore, we checked the impact of various flow rates of the carrier phase, F (in the range from 0.05 [ml/min] to 1 [ml/min]) on the value of the effective diffusion coefficient.

Table 7. The values of the effective diffusion coefficient, which depends on the association constant for different flow rates, F [ml/min] (velocities [cm/s]), of the carrier phase.

F [ml/min]	V [cm/s]	D_{eff} [m ² /s]
1	31	2.28×10^{-10}
0.8	25	2.27×10^{-10}
0.6	19	2.30×10^{-10}
0.4	13	2.24×10^{-10}
0.05	1.5	2.07×10^{-10}

However, we did not observe any significant differences in the effective diffusion coefficient of a ligand in the presence of the macromolecule at different flow rates. It means that the substances are not stretched by the flow characteristically for each flow rate. Consequently, the concentration of macromolecule which is available for the ligand is similar for each flow rate.

6.1.4 Changes of the macromolecule concentration

The next step was to conduct experiments for various concentrations of bovine serum albumin. The key here is to find effective concentration of the macromolecule (see Figure 23). As an example in the experiments we used warfarin. The results provided us with an estimation of changes of the macromolecule concentration during the flow. We observed the following dependence, as shown in Fig 24.

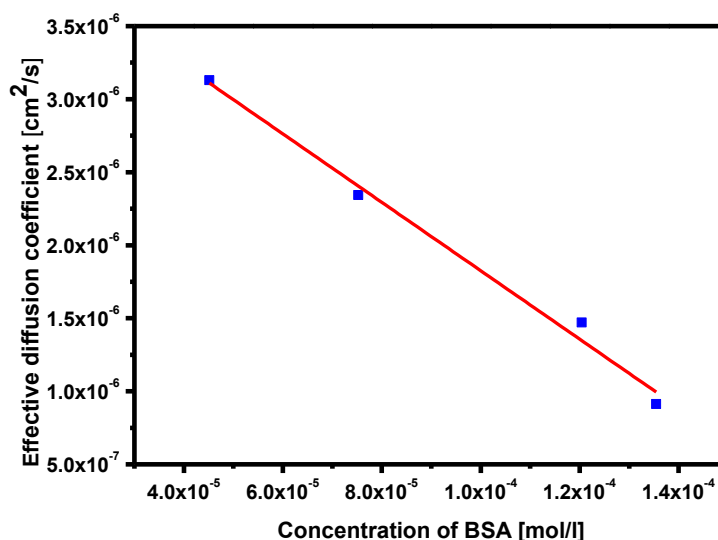


Figure 24. A dependence of effective diffusion coefficient, D_{eff} on the concentrations of bovine serum albumin. The experiments were conducted at a high flow rate, 31 cm/s.

We cannot estimate the changes of the macromolecule concentration during the flow from our experiments, because the changes are random. For an in-depth analysis of these changes, the data should be visualized by i.e. computer simulations.

6.1.5 Changes in the concentration of compounds

In the next step of the experiment we change the concentrations of the compounds. We test different combinations of equilibrium concentrations of ligand and macromolecule. We also check the impact of the ratio of the concentration of the complex at equilibrium to the concentration of free ligand at equilibrium on the effective diffusion coefficient in single injection experiment.

Equilibrium concentrations of the compounds are calculated from the relation (5.4.2).

Table 8. The concentrations of the ligand in the injected sample, the macromolecule in the injection, the complex at equilibrium, the free ligand at equilibrium, the free macromolecule at equilibrium. Comparison of the diffusion coefficient, D , of several drugs determined by flow injection method at high flow rate (31 cm/s) in the buffer solution to the diffusion coefficients, D , of these compounds obtained in a single injection experiment (without filling the capillary). The equilibrium concentrations were calculated using the association constants determined in experiments in which the capillary was filled with the macromolecule solution (sulindac - BSA system $K_a=1.03\times 10^5$, cefaclor - BSA system $K_a=4.45\times 10^3$, etodolac - BSA system $K_a=1.00\times 10^5$, fenbufen - BSA system $K_a=4.17\times 10^5$, diflunisal - BSA system $K_a=1.58\times 10^6$).

Compound	$C_{L(initial)}$ [M]	C_M^0 [M]	C_{LM}^{eq} [M]	C_L^{eq} [M]	C_M^{eq} [M]	D in the buffer solution	D^{eff} in single injection experiment (with BSA)
Sulindac	5.61×10^{-5}	9.03×10^{-6}	7.49×10^{-6}	4.86×10^{-5}	1.54×10^{-6}	3.47×10^{-6}	3.03×10^{-6}
Cefaclor	8.98×10^{-4}	9.03×10^{-6}	7.21×10^{-6}	8.91×10^{-4}	1.82×10^{-6}	3.78×10^{-6}	3.29×10^{-6}
Etodolac	3.48×10^{-4}	9.03×10^{-6}	8.77×10^{-6}	3.39×10^{-4}	2.59×10^{-7}	4.06×10^{-6}	3.40×10^{-6}
Fenbufen	7.87×10^{-4}	9.03×10^{-6}	9.00×10^{-6}	7.77×10^{-4}	2.78×10^{-8}	4.59×10^{-6}	4.75×10^{-6}
Diflunisal	1.60×10^{-4}	9.03×10^{-6}	8.99×10^{-6}	1.51×10^{-4}	3.77×10^{-8}	5.26×10^{-6}	3.30×10^{-6}

The differences between the diffusion coefficient D in the buffer solution and diffusion coefficient D^{eff} with BSA (in single injection experiment) are quite big. It means that in a single injection experiment observation of ligand-macromolecule interaction is possible (Table 8). It confirms results obtained in the subsection 6.1.2 (the differences between diffusion coefficient in the buffer solution and effective diffusion coefficient with BSA are quite large).

Table 9. The concentrations of the complex at equilibrium, C_{LM}^{eq} ; the free ligand (of several drugs) at equilibrium, C_L^{eq} ; and the ratio of these two concentrations, C_{LM}^{eq} to C_L^{eq} . The measurements were conducted at high flow rate, 31 cm/s.

Compound	C_{LM}^{eq} [M]	C_L^{eq} [M]	The ratio of C_{LM}^{eq} to C_L^{eq}
Sulindac	7.49×10^{-6}	4.86×10^{-5}	0.15
Cefaclor	7.21×10^{-6}	8.91×10^{-4}	0.01
Etodolac	8.77×10^{-6}	3.39×10^{-4}	0.03
Fenbufen	9.00×10^{-6}	7.77×10^{-4}	0.01
Diflunisal	8.99×10^{-6}	1.51×10^{-4}	0.06

If the ratio of $\frac{C_{LM}^{eq}}{C_L^{eq}}$ is higher, a larger number of complexes are created. This shows that the changes of the concentration of compounds affect the measurements. However, the number of complexes have to be sufficient to observe the differences between the widths of the peak of free and bound ligands (a situation similar to experiments with filling the whole capillary with the macromolecule solution).

Table 10. The concentrations of the ligand in the injection, $C_{L(\text{initial})}$ the macromolecule in the injected sample, C_M^0 the complex at equilibrium, C_{LM}^{eq} the free ligand at equilibrium, C_L^{eq} the free macromolecule at equilibrium of the sulindac-BSA system as an example. The ratio of the concentration of the complex at equilibrium C_{LM}^{eq} to the concentration of the free ligand at equilibrium, C_L^{eq} . The equilibrium concentrations of the sulindac-BSA system were calculated as in the Table 8. The measurements were conducted at high flow rate, 31 cm/s.

Sulindac			
$C_{L(\text{initial})}$ [M]	5.61×10^{-5}	1.12×10^{-4}	1.12×10^{-4}
C_M^0 [M]	9.03×10^{-6}	9.03×10^{-6}	1.20×10^{-4}
C_L^{eq} [M]	4.86×10^{-5}	1.04×10^{-4}	2.56×10^{-5}
C_M^{eq} [M]	1.54×10^{-6}	7.92×10^{-7}	3.38×10^{-5}
C_{LM}^{eq} [M]	7.49×10^{-6}	8.24×10^{-6}	8.66×10^{-5}
The ratio C_{LM}^{eq} to C_L^{eq}	0.15	0.08	3.38
D in the buffer solution	3.47×10^{-6}	3.47×10^{-6}	3.47×10^{-6}
D^* in a single injection experiment (with BSA)	3.03×10^{-6}	3.16×10^{-6}	1.94×10^{-6}

The differences between the diffusion coefficient D in the buffer solution and the diffusion coefficient D^{eff} in a single injection experiment (with BSA) are much larger when the ratio of the concentration of the complex at equilibrium C_{LM}^{eq} to the concentration of the free ligand at equilibrium C_L^{eq} is higher (Table 10). This confirms that in the case when the ratio C_{LM}^{eq} to C_L^{eq} is equal to 3.38, the number of complexes is sufficient (the higher ratio of $\frac{C_{LM}^{\text{eq}}}{C_L^{\text{eq}}}$, the larger number of complexes) to observe the

differences between the widths of the peaks of free and bound ligands (dispersion coefficient σ is inversely proportional to the diffusion coefficient).

6.1.6 Modifications of the equation

We tested several modifications of the equation (6.1.1). The measurements were conducted at high flow rate, $u=31$ cm/s. We checked all modifications of the equation (6.1.1) based on the sulindac-BSA system. Originally we used the following equation, which we decided to modify:⁷¹

$$K_a = \frac{(D^{eff} - D_L)}{(D_M - D^{eff})c_M} \quad (6.1.1)$$

where D_{eff} is effective diffusion coefficient [$\frac{cm^2}{s}$] of the ligand interacting with macromolecule, D_L is the diffusion coefficient [$\frac{cm^2}{s}$] of the free ligand, D_{LM} [$\frac{cm^2}{s}$] is the diffusion coefficient of the macromolecule, K_a is the association constant [M^{-1}], and c_M is the concentration of the macromolecule solution.

The concentrations of the reagents at equilibrium were calculated from the following relation:

$$K_a = \frac{C_{LM}^{eq}}{C_{L(final)} - C_{LM}^{eq}} (C_P^0 - C_{LM}^{eq}) \quad (6.1.2)$$

where K_a is the association constant; C_{LM}^{eq} is the concentration of the complex at equilibrium; $C_{L(final)}$ is the overall concentration of the ligand at the capillary's end; and C_M^0 is the overall concentration of the macromolecule.

Table 11. Modifications of the equation (7.2.1) for sulindac-BSA system. The concentration of the drug was $c_L = 1.12 \times 10^{-4}$ in all experiments. The concentrations of BSA were as follows: $c_M = 4.52 \times 10^{-5}$, $c_M = 7.53 \times 10^{-5}$, $c_M = 1.20 \times 10^{-4}$, $c_M = 1.35 \times 10^{-4}$ [M]. The association constant K_a obtained from the equation (6.1.1) for each concentration were as follows: $K_a = 6.19 \times 10^3$, $K_a = 8.56 \times 10^3$, $K_a = 7.35 \times 10^3$, $K_a = 1.02 \times 10^4$ [M^{-1}].

K_a for $c_M = 4.52$ $\times 10^{-5}$ [M^{-1}]	K_a for $c_M = 7.53$ $\times 10^{-5}$ [M^{-1}]	K_a for $c_M = 1.20$ $\times 10^{-4}$ [M^{-1}]	K_a for $c_M = 1.35$ $\times 10^{-4}$ [M^{-1}]	Modified equations
9.73×10^4	5.28×10^4	3.57×10^4	2.47×10^4	$c_M = C_M^{eq}; K_a = \frac{(D^{eff} - D_L)}{(D_M - D^{eff})C_M^{eq}}$
1.21×10^4	1.21×10^4	6.23×10^3	7.46×10^3	$c_M = C_M^{eq} \frac{\sigma_M}{\sigma_L}; K_a = \frac{(D^{eff} - D_L)}{(D_M - D^{eff})C_M^{eq} \frac{\sigma_M}{\sigma_L}}$
1.46×10^3	2.02×10^3	1.74×10^3	2.41×10^3	$c_M = c_M \frac{\sigma_M}{\sigma_L}; K_a = \frac{(D^{eff} - D_L)}{(D_M - D^{eff})c_M \frac{\sigma_M}{\sigma_L}}$
2.48×10^4	2.48×10^4	1.28×10^4	1.53×10^4	$c_M = C_M^{eq} \sqrt{\frac{\sigma_M}{\sigma_L}}; K_a = \frac{(D^{eff} - D_L)}{(D_M - D^{eff})C_M^{eq} \sqrt{\frac{\sigma_M}{\sigma_L}}}$
3.01×10^3	4.16×10^3	3.57×10^3	4.96×10^3	$c_M = c_M \sqrt{\frac{\sigma_M}{\sigma_L}}; K_a = \frac{(D^{eff} - D_L)}{(D_M - D^{eff})c_M \sqrt{\frac{\sigma_M}{\sigma_L}}}$
6.89×10^3	9.53×10^3	8.18×10^3	1.14×10^4	$c_M = c_M \sqrt{\frac{\sigma_{eff}}{\sigma_L + \sigma_{eff}}}; K_a = \frac{(D^{eff} - D_L)}{(D_M - D^{eff})c_M \sqrt{\frac{\sigma_{eff}}{\sigma_L + \sigma_{eff}}}}$
5.68×10^4	5.69×10^4	2.93×10^4	3.51×10^4	$c_M = C_M^{eq} \sqrt{\frac{\sigma_{eff}}{\sigma_L + \sigma_{eff}}}; K_a = \frac{(D^{eff} - D_L)}{(D_M - D^{eff})C_M^{eq} \sqrt{\frac{\sigma_{eff}}{\sigma_L + \sigma_{eff}}}}$

^s correct value for sulindac-BSA system is equal to $K_a = 1.00 \times 10^5$.

Where C_M^{eq} is the concentration of the macromolecule solution at equilibrium; σ_M is the dispersion coefficient (the width of the concentration distribution) of the macromolecule, σ_L is the dispersion coefficient of the ligand, and σ_{eff} is the effective dispersion coefficient.

The results indicate that the best accordance of K_a obtained from previous experiments (for sulindac $K_a = 1.00 \times 10^5$) and K_a calculated from the equations was achieved for the first equation (Table 11) and $c_M = 4.52 \times 10^{-5}$ M. In this equation, instead of using the concentration of the macromolecule c_M the concentration of the macromolecule at equilibrium C_M^{eq} was used. The value of the association constant (obtained from the modified equation) which is similar to the value of the association constant obtained from equation 6.1.1, is marked in the Table 11 by red colour.

This part of the thesis shows that observation of interactions in a single injection experiment is possible but still requires computer simulations and improvement of the existing theory.

7. Surfactant–dye interactions

7.1 Surfactants

Another complex system considered in this work is the solution of surfactants. Surfactants are composed of a hydrophobic part (uncharged carbohydrate group) and a hydrophilic part. A hydrophilic head of the surfactant can be classified as anionic, non-ionic or cationic. One of the most popular anionic surfactants is sodium dodecyl sulfate (SDS). Hexaethylene glycol monododecyl ether (C12E6) represents the

uncharged surfactant while cetyltrimethylammonium chloride (CTAC) belongs to the category of cationic surfactants.

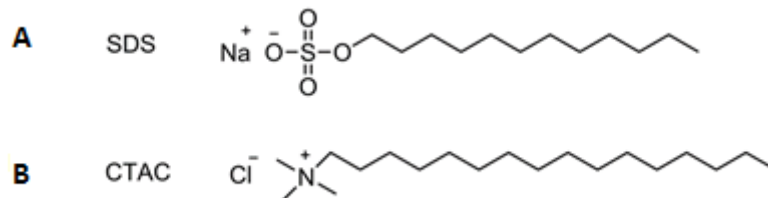


Figure 25. (A) A chemical structure with negatively charged head (SDS) and (B) a chemical structure with positively charged head (CTAC).

The molecules of the surfactants have a tendency to organize themselves. Self-assembly of the surfactant molecules leads to the formation of micelles. Surfactant molecules form micelles above a specific concentration, called the critical micelle concentration (CMC). The concentration of micelles, C_m , can be calculated from the surfactant concentrations C_s as follows:^{79,80}

$$C_m = \frac{C_s - \text{CMC}}{N_{\text{ag}}} \quad (7.1.1)$$

Where: N_{ag} is the mean number of aggregated surfactant molecules.

7.2 Formation of the micelle-dye complex: theory

Noncovalent interactions of the dyes with the micelles play a crucial role in the understanding of kinetic processes of many biochemical and chemical reactions. Studies of dye–surfactant interactions (Figure 26) provide a lot of valuable information concerning their industrial applications. Moreover, the complexity of micellar exchange is significant in planning of surfactant solutions in technological processes such as solubilization, foaming, wetting and detergency.

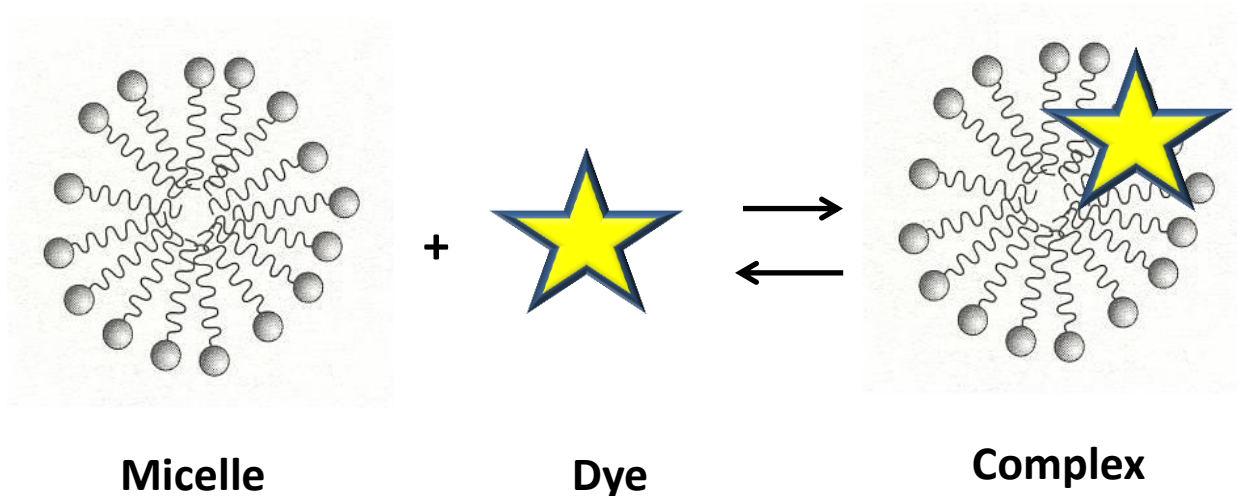


Figure 26. A schematic representation of association and dissociation of a dye with a micelle.

The noncovalent interactions between dye and micelles can be treated as chemical reactions with the association constant K_a :

$$A + B \xrightleftharpoons{K_a} C, K_a = \frac{k_{on}}{k_{off}} = \frac{[C]}{[A][B]} \quad (7.2.1)$$

Where: [A], [B], [C] is the concentration of the micelle, free dye and micelle-dye complex at equilibrium respectively; k_{on} and k_{off} are association and dissociation rate constants of the formation of the complex.

The concentration of micelles is always much higher than the concentration of the dye, $[M] \gg [D] \approx 10^{-9}$ M. Therefore, we defined D_{eff} as follows:

$$D_{eff} = \frac{D_{dye}t_{dye} + D_{complex}t_{complex}}{t_{dye} + t_{complex}} \quad (7.2.2)$$

Where D_{dye} is the diffusion coefficient of free dye, $D_{complex}$ is the diffusion coefficient of dye-micelle complex, t_{dye} is the time spent in the free state, and $t_{complex}$ is the time spent in the bound state.

The ratio of the molar concentration of free dye, [B], and complex, [C], is related to the association constant:

$$K_a[A] = \frac{[C]}{[B]} = \frac{t_{complex}}{t_{dye}} \quad (7.2.3)$$

Combining equation (7.2.2) and equation (7.2.3), we finally get:^{80,81}

$$K_a = \frac{D_{eff} - D_{dye}}{(D_{complex} - D_{eff})[A]} \quad (7.2.4)$$

7.3 Interactions of rhodamine 110 with cationic surfactant cetyltrimethylammonium chloride (CTAC)

We checked diffusion of rhodamine 110 in two different concentrations of cationic surfactant (CTAC) solutions $C_s = 2.50 \times 10^{-3}$ M and 6.20×10^{-3} M. We determined a diffusion coefficient of a free dye in water and a diffusion coefficient of the dye in the presence of the surfactant. The concentration of the dye was $C_d = 1.10 \times 10^{-4}$ M and it was constant during all measurements. The diffusion coefficient of a free surfactant was obtained using Dynamic Light Scattering (DLS) technique as the surfactant does not absorb UV-Vis light. For the measurements we used high flow rate (31 cm/s) and long, coiled capillaries (the procedure is the same as in previous study). Formation of micelles was ensured by using concentrations of the surfactants above critical micelle concentration (CMC). A critical micelle concentration (CMC) for surfactant at 25 °C was 1.25×10^{-3} M. Absorption wavelength for rhodamine (Figure 27) was 496 nm.

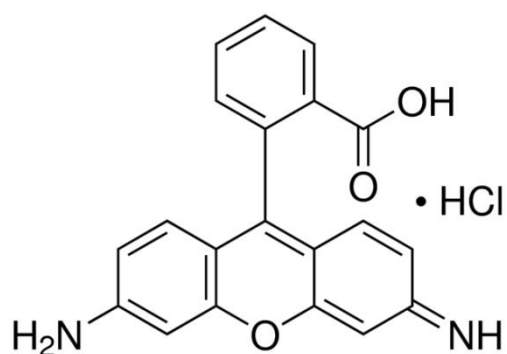


Figure 27. Chemical structure of rhodamine 110.⁸²

Table 12. Values of diffusion coefficients of a free dye in water, a free surfactant and the diffusion coefficient of the dye in a presence of cationic surfactant for two different concentrations of the surfactant.

Substance	D [m ² /s] for a surfactant concentration of C _s =2.50×10 ⁻³ M	D [m ² /s] for a surfactant concentration of C _s =6.20×10 ⁻³ M
Surfactant CTAC	0.80×10 ⁻¹⁰ *	0.84×10 ⁻¹⁰ *
Rhodamine in a presence of surfactant CTAC	2.58×10 ⁻¹⁰	1.53×10 ⁻¹⁰

The diffusion coefficient of rhodamine in water was equal to D = 3.70×10⁻¹⁰ m²/s.

* Values of the diffusion coefficients were taken from DLS measurements.

The value of the association constant for the concentration of cationic surfactant $C_s = 2.50 \times 10^{-3}$ M was $K_a = 4.03 \times 10^{-4}$ M⁻¹. The value of the association constant for the concentration of the surfactant $C_s = 6.20 \times 10^{-3}$ M was $K_a = 5.08 \times 10^{-4}$ M⁻¹. The actual value of the association constant was an average of association constants obtained for these two concentrations for Rh110–CTAC system and was equal to $K_a = 4.55 \times 10^{-4}$ M⁻¹. This value of the association constant demonstrates that the interactions observed in the studied dye-micelle system are quite strong. The dye-micelle interaction is caused by hydrophobic and electrostatic force. CTAC has many alkyl groups which are responsible for hydrophobic interaction. However, the high affinity of the zwitterionic dye rhodamine 110 (Figure 19) to the CTAC micelles is caused by the electrostatic interactions. Rh110 carries a positive charge due to the presence of carboxyl groups and a negative charge due to the presence of amino groups. The results show that our method can potentially facilitate the physicochemical studies of dye-micelle interactions.

7.4 Interactions of atto 488 with anionic surfactant sodium dodecyl sulfate (SDS)

We determined the diffusion coefficient of atto 488 in water. The measurements were conducted at high flow rates of a carrier phase, 31 cm/s. Additionally, values of diffusion coefficients were obtained at low flow rate of the carrier phase - 1.5 cm/s. The experiments on the atto 488–SDS system were conducted for three different concentrations of surfactants, $c_s = 3.12 \times 10^{-2}$ M, $c_s = 1.60 \times 10^{-2}$ M and $c_s = 9.40 \times 10^{-3}$ M. The diffusion coefficients of the dye in the presence of surfactant solutions were also determined. The concentration of the dye was constant during all measurements and equal to $c_d = 3.30 \times 10^{-4}$ M. The diffusion coefficient of the surfactant (SDS) was

collected from dynamic light scattering measurements. Concentration of the anionic surfactant was higher than the critical micelle concentration (CMC). The critical micelle concentration (CMC) of the surfactant at 25 °C was 8×10^{-3} M. The absorption wavelength for atto 488 was 523 nm (see Fig.28).

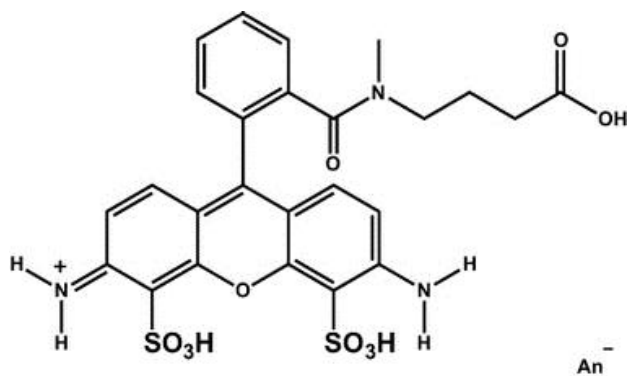


Figure 28. The chemical structure of Atto 488. Atto 488 is a labeling dye designed for high sensitivity applications - for example a single molecule detection.⁸⁰

Table 13. Values of diffusion coefficients of free dye in water, free micelles and a diffusion coefficient of the dye in the presence of anionic surfactant for three different concentrations of the surfactant at high flow rate, 31 cm/s.

Substance	Diffusion coefficient, D [m ² /s] for the surfactant concentration of C _s =3.12×10 ⁻² M	Diffusion coefficient, D [m ² /s] for the surfactant concentration of C _s =1.60×10 ⁻² M	Diffusion coefficient, D [m ² /s] for the surfactant concentration of C _s =9.40×10 ⁻³ M
Surfactant SDS	0.97×10 ⁻¹⁰ *	0.97×10 ⁻¹⁰ *	0.94×10 ⁻¹⁰ *
Atto 488 in the presence of surfactant SDS	3.30×10 ⁻¹⁰	3.39×10 ⁻¹⁰	3.42×10 ⁻¹⁰

The diffusion coefficient of Atto 488 in water was equal to D = 3.39×10⁻¹⁰ m²/s.

* Values of diffusion coefficients were taken from DLS measurements.

Table 14. Values of diffusion coefficients of free dye in the water, free micelles and the diffusion coefficient of the dye in the presence of anionic surfactant for three different concentrations of the surfactant at low flow rate, 1.5 cm/s.

Substance	D [m ² /s] for the surfactant concentration of C _s =3.12×10 ⁻² M	D [m ² /s] for the surfactant concentration of C _s =1.60×10 ⁻² M	D [m ² /s] for the surfactant concentration of C _s =9.40×10 ⁻³ M
Surfactant SDS	0.97×10 ⁻¹⁰ *	0.97×10 ⁻¹⁰ *	0.94×10 ⁻¹⁰ *
Atto 488 in the presence of surfactant SDS	3.95×10 ⁻¹⁰	3.95×10 ⁻¹⁰	3.95×10 ⁻¹⁰

The diffusion coefficient of Atto 488 in water was equal to $D = 3.69 \times 10^{-10} \text{ m}^2/\text{s}$.

* Values of diffusion coefficients were taken from DLS measurements.

The results in Table 13 and 14 show that the differences between a diffusion coefficient of a free dye and a diffusion coefficient of the dye in the presence of the surfactant SDS are very small. It means that interaction between Atto 488 and SDS is very weak. The measurements at high flow rates (Table 13) show that the value of the diffusion coefficient of free dye is similar to the value of the diffusion coefficient of the dye in presence of SDS. The diffusion coefficients of the surfactant SDS (DLS) have similar value for all concentrations (Table 13 and 14). The measurements included in the Table 13 show that we cannot observe any interactions (the diffusion coefficients of Atto 488 in the presence of SDS have the same values). However, we also conducted the measurements at low flow rates. We wanted to give the molecules more time to interact with each other. The results (Table 14) show that the diffusion coefficient of the

dye obtained at low flow rates is higher in water than the diffusion coefficient determined at high flow rates. These differences can be related to the partial adsorption process of the dye in the quartz window. The dye has much more time for an adsorption at low flow rates (about 50 minutes). The diffusion coefficient of Atto 488 in the presence of the surfactant SDS obtained at low flow rates is also higher than the diffusion coefficient of the Atto 488-SDS system determined at high flow rates. However, all measurements indicate that the interactions between Atto 488 and SDS are too weak. It is obvious that in this case we cannot obtain the value of the association constant.

8. Protein-DNA interactions

8.1 Protein-DNA interactions: the aim of this work

The aim of this part of my work was to study the binding of a member of the IRF (Interferon Regulatory Factor) family to a known and specific DNA binding site (called ISRE: Interferon Stimulated Response Element) present in many IFN (Interferon) inducible genes. Interferon regulatory factors are proteins which regulate a transcription of interferons. We had samples with oligonucleotides (a), a nuclear extract without over-expressing IRF9 (Interferon regulatory factor 9 is a protein which in humans is encoded by the IRF9 gene) (b) and a sample with a nuclear extract containing over-expressing IRF9 (c). We wanted to determine the values of diffusion coefficients for these three different samples. We conducted experiments to check if IRF9 interacts with the DNA (the interaction of DNA with IRF9 slows down DNA diffusion).⁸³

8.2 Description of the experiment

We prepared three samples:

- a) Oligonucleotides
- b) U3C – cell line (nuclear extract)
- c) IRF9 – U3C – nuclear extract with over-expressing IRF9

Oligonucleotides:

Sequence 1 (5' => 3') **GGC TTC AGT TTC GGT TTC CCT TTC CCG AG**

Sequence 1 (3' => 5') **CCG AAG TCA AAG CCA AAG GGA AAG GGC TC-TAMRA**

Preparation of the oligonucleotides:

1. Assembling the oligonucleotides at the bottom of the tube by a short spin (about 5 minutes).
2. Diluting the oligonucleotides in TE buffer (10mM Tris, pH=8; 0.1 mM EDTA pH=8).
3. Heating the oligonucleotides in 95 °C for 4 minutes.
4. Leaving the oligonucleotides in room temperature (to cool down very slowly).
5. Conducting experiments with the oligonucleotides in sterile conditions.

Sample 1

DNA

20 µl nucleotides + 200 µl lysis buffer + 200 µl sterile water + 40 µl binding buffer + 20 µl MgCl₂ + 20 µl NP40

Sample 2

Extract without interacting protein (IRF9)

20 µl nucleotides + 200 µl U3C + 200 µl sterile water + 40 µl binding buffer + 20 µl MgCl₂ + 20 µl NP40

Sample 3

Extract with interacting protein (IRF9)

20 µl nucleotides + 200 µl IRF9-U3C + 200 µl sterile water + 40 µl binding buffer + 20 µl MgCl₂ + 20 µl NP40

Binding Buffer:

100 mM Tris, 500 mM KCl, 10 mM DTT, pH = 7.5

NP-40:

Nonylphenyl Polyethylene Glycol. It is a commercially available detergent. NP-40 is a solubilizing agent interacting with membrane proteins and lipids.

DTT:

DL-Dithiothreitol. It is used to stabilize enzymes and other proteins. DTT quantitatively reduces disulfide bonds.

MgCl₂:

The ions are important for specific promoter function.

8.3 Results and conclusions

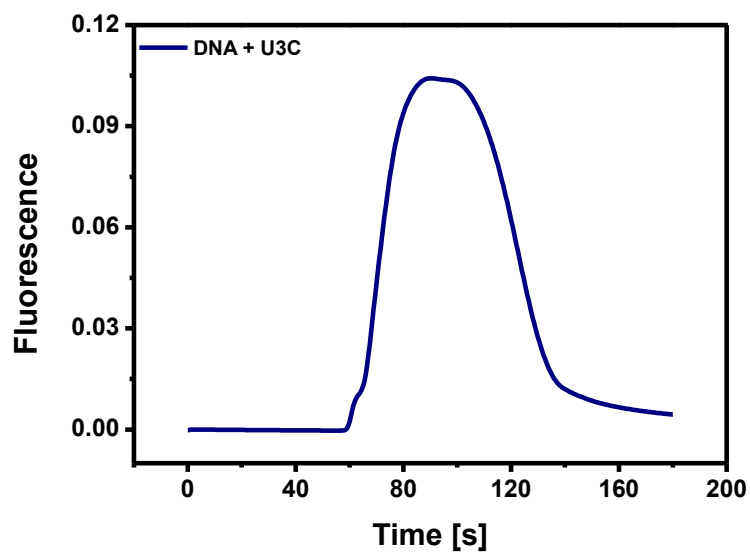


Figure 29. Fluorescence of DNA (oligonucleotides are labeled with TAMRA) with nuclear extract as a function of time at high flow rate, $u = 30$ cm/s, L equals ~ 30 m long capillary. The excitation wavelength was $\lambda_{Ex} = 546$ and the emission wavelength was $\lambda_{Em} = 579$. The distribution is shown for the second sample – the extract without interacting protein.

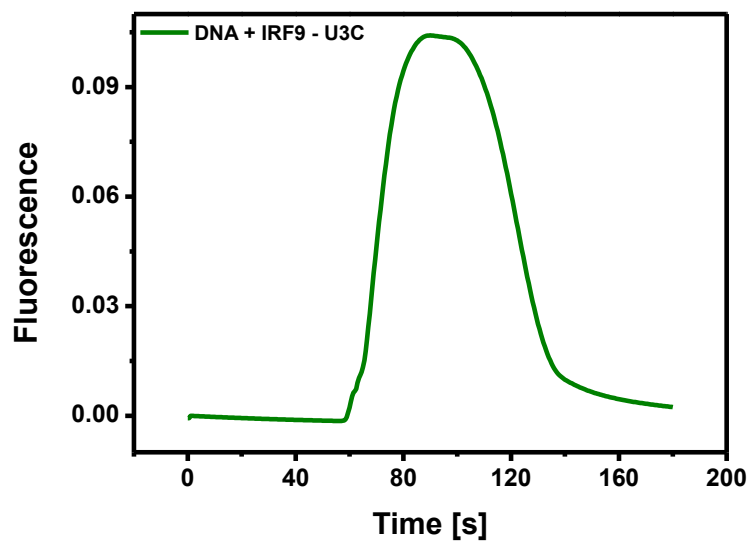


Figure 30. A fluorescence of DNA (oligonucleotides are labeled with TAMRA) with nuclear extract and interacting IRF9 as a function of time at high flow rate, $u = 30$ cm/s, L equals ~ 30 m long capillary. The excitation wavelength was $\lambda_{Ex} = 546$ and the emission wavelength was $\lambda_{Em} = 579$. The distribution is shown for the third sample – the extract with interacting protein.

A proper analysis of the experimental results cannot be carried out because of the incorrect shape of the peaks. We suspect that not all of the strands are in the form of double stranded DNA after the reaction (conducted according to the protocol).

9. Summary and conclusions

In my dissertation I present a new flow injection method for determination of the association constants of ligand–macromolecule complex formation. The method is based on determining the width of the concentration distribution of the complexes forming compounds.

In the first part of the experimental section I present the results of my study of interactions between compounds of known association constants (drug-BSA). The results were in strong agreement with the literature data. I also determined association constants of 3β- and 3α-aminotropane ligands of 5-HT1A, 5-HT2A and D2 receptors with the bovine serum albumin (BSA). I studied the range of different values of K_a . I confirmed that the flow injection method is useful when studying K_a for a wide range of values from 10^2 to 10^9 M^{-1} . I established that the range of the studied values of the association constant depends on the concentration of the macromolecule, the concentration of the ligand, the volume of the capillary, the volume of the injection and the accuracy of the measurements (sensitivity of the UV–vis detector). I demonstrated that this method of determining formation of a protein–drug complex is fast and flexible, as determination of K_a takes less than 9 minutes. The thermodynamic properties of the process such as ionic strength, temperature and viscosity can be changed easily.

The aim of the second part of my work was to decrease the amount of solutions used in the experiments. In the new version of the experiments we injected a ligand with a macromolecule in a single injection into a buffer solution. A complex was formed

during the flow. In this part of the work I showed that we can eliminate the overlapping of the peaks (caused by absorption of the compounds at similar wavelengths). I proved that differences between diffusion coefficients of the free and bound ligand in a single injection experiment are sufficient to estimate the value of the association constant (difference between values is up to 60%). I assume concentration changes for different flow rates (31cm/s -1.5 cm/s). I tested different conditions (i.e. various concentrations of BSA: $c_M = 4.52 \times 10^{-5}$, $c_M = 7.53 \times 10^{-5}$, $c_M = 1.20 \times 10^{-4}$, $c_M = 1.35 \times 10^{-4}$) and modifications of the equation which allowed me to describe a single injection experiment. However, the experiments presented in the second part of my thesis need to be studied using computer simulations and require improvements of the existing theory. Thus this subject will be further investigated.

In the next part of my dissertation I briefly described surfactants and creation of a dye-micelle system. I studied interactions of rhodamine 110 with CTAC and determined the value of the association constant for this system. The studies show that these kinds of interactions are quite strong ($K_a = 4.55 \times 10^4 \text{ M}^{-1}$). However, for the next studied dye-micelle system - Atto 488 with SDS - the measurements indicate that the interactions are too weak. We could not detect any interactions between this dye the micelles.

In the last part of my thesis I considered protein-DNA interactions. In this study I tried to estimate a binding of a member of Interferon Regulatory Factor to a known and specific DNA binding site called Interferon Stimulated Response Element. It possesses cells without (U3C) and over-expressing IRF9 (IRF9-U3C). Nevertheless, these experiments could not be analyzed properly because of non-symmetric shape of the peak. The reason for such behavior is that not all of the strands connect together to make the double helix shape of DNA.

The method proposed in this thesis opens a new avenue for similar studies in analytical chemistry. I am convinced that our technique will in the future replace other methods (i.e. dialysis, ultrafiltration, ultracentrifugation and electrophoresis) used for studying of formation of the ligand-macromolecule complexes.

In summary, the most important results of my PhD thesis are:

- The flow injection method was used for determination of an association constant for drug-BSA systems. The results were in strong agreement with those presented in the literature
- The association constants of 3β- and 3α-aminotropane ligands of 5-HT1A, 5-HT2A and D2 receptors with the bovine serum albumin (BSA) were obtained
- The parameters which influence the association constant were determined
- The flow injection method can be used to study a wide range of K_a from 10^2 to 10^9 M^{-1}
- The basis for the experiment conducted during single injection (ligand with macromolecule) was created
- The method can be used for studying the dye-micelle systems
- The procedure of studying the protein-DNA interactions requires improvement

10. References

- [1] Y. N. E. Eman, “Gravitational interaction of hadrons : Band-spinor representations of $GL(n, R)$,” *Proc. Natl. Acad. Sci.* vol. 74, no. 10, pp. 4157–4159, **1977**.
- [2] C. Mastropietro, B. Moore, L. Mayer, J. Wadsley, J. Stadel, “The gravitational and hydrodynamical interaction between the Large Magellanic Cloud and the Galaxy,” *Mon. Not. R. Astron. Soc.*, vol. 363, no. 2, pp. 509–520, **2005**.
- [3] A. Salam, J. C. Ward, “Electromagnetic and weak interactions,” *Phys Lett.* vol. 13, no. 2, pp. 168-176, **1964**.
- [4] K. Mursula, M. Roos, F. Scheck, “The Lorentz structure of leptonic charged weak interactions,” *Nucl Phys B.*, vol. 219, no. 2, pp. 321–340, **1983**.
- [5] D. H. Kobe, A.E. Smirl, “Gauge invariant formulation of the interaction of electromagnetic radiation and matter,” *Am. J. Phys.*, vol. 46, no. 6, pp. 624-633, **1978**.
- [6] Y. Ne'eman, “Derivation of strong interactions from a gauge invariance ,” *Nucl Phys B.*, vol. 26, no. 2, pp. 222–229, **1961**.
- [7] R. G. Burns, M. Application, C. G. Kalodimos, N. Biris, A. M. J. J. Bonvin, M. M. Levandoski, M. Guennuegues, R. Boelens, R. Kaptein, “Structure and Flexibility Adaptation in Nonspecific and Specific Protein-DNA Complexes,” *Science*, vol. 305, no. July, pp. 386–389, **2004**.
- [8] R. P. Bahadur, P. Chakrabarti, F. Rodier, J. Janin, “A Dissection of Specific and Non-specific Protein-Protein Interfaces,” *J. Mol. Biol.*, vol. 336, no. 4, pp. 943–955, **2004**.
- [9] Y. Zhang, Y. Li, and W. Liu, “Dipole-Dipole and H-Bonding Interactions Significantly Enhance the Multifaceted Mechanical Properties of Thermoresponsive Shape Memory Hydrogels,” *Adv. Funct. Mater.*, vol. 25, no. 3, pp. 471–480, **2015**.
- [10] F. London, “The general theory of molecular forces.,” *Trans. Faraday Soc.*, vol. 35, no. 8, pp. 8–26, **1937**.

- [11] I. Langmuir, "The Role of Attractive and Repulsive Forces in the Formation of Tactoids, Thixotropic Gels, Protein Crystals and Coacervates," *J. Chem. Phys.* vol. 873, no. 6, pp. 873-897, **1938**.
- [12] J. A. Lemkul, J. Huang, A. D. MacKerell, "Induced Dipole-Dipole Interactions Influence the Unfolding Pathways of Wild-Type and Mutant Amyloid β -Peptides," *J. Phys. Chem. B* vol. 119, no. 8, pp. 15574–15582, **2015**.
- [13] J. T. Broussard, "Multipole Polarizabilities and London Dispersion Forces of He and Li+ Using Double Perturbation Theory," *J. Chem. Phys.* vol. 53, no. 4, pp. 1507-1510, **1970**.
- [14] M. J. Stephen, "First-Order Dispersion Forces," *J. Chem. Phys.* vol. 40, no. 3, pp. 669–673, **1964**.
- [15] W. L. Bade, "Drude model calculation of dispersion forces. I. General theory," *J. Chem. Phys.* vol. 27, no.6, pp. 1280–1284, **1957**.
- [16] R. H. French, "Origins and Applications of London Dispersion Forces and Hamaker Constants in Ceramics," *J. Am. Ceram. Soc.* vol. 83, no.9, pp. 2117-2146, **2000**.
- [17] P. Demontis, S. Spanu, G. B. Suffritti, P. Demontis, S. Spanu, G. B. Suffritti, "Application of the Wolf method for the evaluation of Coulombic interactions to complex condensed matter systems: Aluminosilicates and water," *J. Chem. Phys.* vol. 114, no. 18, pp. 7980-7988, **2001**.
- [18] M. Bostrom, D. R. M. Williams, B. W. Ninham, "Ion specificity of micelles explained by ionic dispersion forces," *Langmuir* vol. 18, no. 21, pp. 6010–6014, **2002**.
- [19] A. Garem, G. Daufin, J. Maubois, B. Chaufer, J. Leonil, "Ionic interactions in nanofiltration of beta casein peptides," *Biotechnol. Bioeng.* vol. 57, no. 1, pp. 109–117, **1997**.
- [20] A. R. Fersht, J.-P. Shi, J. Jones, D. M. Lowe, A. J. Wilkinson, D. M. Blow, P. Brick, P. Carter, M. M. Y. Waye, G. Winter, "Hydrogen bonding and biological specificity analysed by protein engineering," *Nature* vol. 314, no. 2, pp. 235–238, **1985**.
- [21] J. V. Barth, J. Weckesser, C. Cai, P. Gunter, L. Burgi, O. Jeandupeux, and K. Kern, "Building supramolecular nanostructures at surfaces by hydrogen bonding," *Angew. Chem. Int. Ed.* vol. 39, no. 7, pp. 1230-1233, **2000**.

- [22] L. F. Scatena, M. G. Brown, G. L. Richmond, "Water at Hydrophobic Surfaces : Weak Hydrogen Bonding and Strong Orientation Effects," *Science* vol. 292, no. 4, pp. 908–912, **2001**.
- [23] G. Hummer, S. Garde, A. E. García, M. E. Paulaitis, L. R. Pratt, "The pressure dependence of hydrophobic interactions is consistent with the observed pressure denaturation of proteins," *Proc. Natl. Acad. Sci.* vol. 95, no. 4, pp. 1552–1555, **1998**.
- [24] D. E. Smith, A. D. J. Haymet, "Free energy, entropy, and internal energy of hydrophobic interactions: Computer simulations," *J. Chem. Phys.* vol. 98, no. 8, pp. 6445-6454, **1993**.
- [25] P. Atkins, J. Paula "Physical Chemistry for the Life Sciences," Oxford, **2006**.
- [26] M. Mihailescu and M. K. Gilson, "On the Theory of Noncovalent Binding," *Biophys. J.* vol. 87, no. 1, pp. 23–36, **2004**.
- [27] R. Benesch, R. E. Benesch, C. I. Yu, "Reciprocal binding of oxygen and diphosphoglycerate by human hemoglobin.," *Proc. Natl. Acad. Sci.* vol. 59, no. 2, pp. 526–532, **1968**.
- [28] J.R. Knowles, W.J. Albery, "Perfection in Enzyme catalysis: The Energetics of Triosephosphate Isomerase," *Acc. Chem. Res.* vol. 10, no. 4, pp. 105–110, **1977**.
- [29] E. Lolis, T. Alber, R. C. Davenport, D. Rose, F. C. Hartman, G. A. Petsko, "Structure of yeast triosephosphate isomerase at 1.9-Å resolution," *Biochemistry* vol. 29, no. 28, pp. 6609–6618, **1990**.
- [30] K. A. Xavier, R. C. Willson, "Association and dissociation kinetics of anti-hen egg lysozyme monoclonal antibodies HyHEL-5 and HyHEL-10.," *Biophys. J.*, vol. 74, no. 4, pp. 2036–2045, **1998**.
- [31] D. Lancet, E. Sadvovsky, E. Seidemann, "Probability model for molecular recognition in biological receptor repertoires: significance to the olfactory system.," *Proc. Natl. Acad. Sci. USA* vol. 90, no. 8, pp. 3715–3719, **1993**.
- [32] K.A. Connors, "Binding constants: The measurement of molecular complex stability," New York, **1987**.
- [33] J. P. Hummel, W. J. Dreyer, "Measurement of protein-binding phenomena by gel filtration.," *Biochim. Biophys. Acta* vol. 63, pp. 530–532, **1962**.

- [34] J. C. Giddings, "Maximum Number of Components Resolvable by Gel Filtration and Other Ellution Chromatographic Methods," *Anal. Chem.* vol. 39, no. 8, pp. 1027–1028, **1967**.
- [35] S. J. Hubert, G. W. Slater, J.-L. Viovy, "Theory of Capillary Electrophoretic Separation of DNA Using Ultradilute Polymer Solutions," *Macromolecules* vol. 29, no. 6, pp. 1006–1009, **1996**.
- [36] R. M. McCormick, "Capillary Zone Electrophoretic Separation of Peptides and Proteins Using Low pH Buffers in Modified Silica Capillaries," *Anal. Chem.* vol. 60, no. 21, pp. 2322–2328, **1988**.
- [37] T. W. Randolph, "Phase separation of excipients during lyophilization: Effects on protein stability," *J. Pharm. Sci.*, vol. 86, no. 11, pp. 1198–1203, **1997**.
- [38] R. G. Harrison, "Protein purification process engineering," New York, **1994**.
- [39] G. M. Verkhivker, D. Bouzida, D. K. Gehlhaar, P. A. Rejto, S. T. Freer, P. W. Rose, "Complexity and simplicity of ligand-macromolecule interactions: The energy landscape perspective," *Curr. Opin. Struct. Biol.* vol. 12, no. 2, pp. 197–203, **2002**.
- [40] R. S. Spolar, M. T. Record, "Coupling of local folding to site-specific binding of proteins to DNA," *Science* vol. 263, no. 5148, pp. 777–784, **1994**.
- [41] S. E. Halford, J. F. Marko, "How do site-specific DNA-binding proteins find their targets?," *Nucleic Acids Res.*, vol. 32, no. 10, pp. 3040–3052, **2004**.
- [42] R. Evans, N. Lipscomb, "The Effect of pH on the Cooperative Behavior of Aspartate Transcarbamylase from *Escherichia coli*," *J. Biol. Chem.* vol. 253, no. 13, pp. 4624–4630, **1978**.
- [43] T. Litman, T. Zeuthen, T. Skovsgaard, W. D. Stein, "Competitive, non-competitive and cooperative interactions between substrates of P-glycoproteins as measured by ATPase activity," *Biochim. Biophys. Acta - Mol. Basis Dis.* vol. 1361, no. 2, pp. 169–176, **1997**.
- [44] M. Wessling-Resnick, G. L. Johnson, "Allosteric behavior in transducin activation mediated by rhodopsin. Initial rate analysis of guanine nucleotide exchange," *J. Biol. Chem.*, vol. 262, no. 8, pp. 3697–3705, **1987**.
- [45] W. A. Lim, "The modular logic of signaling proteins: Building allosteric switches from simple binding domains," *Curr. Opin. Struct. Biol.*, vol. 12, no. 1, pp. 61–68, **2002**.

- [46] J. S. Marvin, E. E. Corcoran, N. A. Hattangadi, J. V. Zhang, S. A. Gere, H. W. Hellinga, "The rational design of allosteric interactions in a monomeric protein and its applications to the construction of biosensors.," *Proc. Natl. Acad. Sci. U.S.A.*, vol. 94, no. 9, pp. 4366–4371, **1997**.
- [47] H. Lodish, A. Berk, C.A. Kaiser, M. Krieger, M. P. Scott, A. Bretscher, H. Ploegh, P. Matsudaira "Molecular Cell Biology," W.H Freeman and Company, **2008**.
- [48] K. Rippe, "Analysis of protein-DNA binding at equilibrium," *BIF Futur.*, vol. 12, no. 1, pp. 20–26, **1997**.
- [49] H. E. Rosenthal, "A graphic method for the determination and presentation of binding parameters in a complex system," *Anal. Biochem.* vol. 20, no. 3, pp. 525–532, **1967**.
- [50] H. G. Weder, J. Schildknecht, R. A. Lutz, P. Kesselring, "Determination of binding parameters from Scatchard plots. Theoretical and practical considerations.," *Eur. J. Biochem.* vol. 42, no. 2, pp. 475–481, **1974**.
- [51] P. Peszynski, S. Klammt, E. Peters, S. Mitzner, J. Stange, and R. Schmidt, "Albumin dialysis: single pass vs. recirculation (MARS).," *Liver* vol. 22, no.2, pp. 40–2, **2002**.
- [52] K. Vuignier, J. Schappler, J.-L. Veuthey, P.-A. Carrupt, and S. Martel, "Drug–protein binding: a critical review of analytical tools," *Anal. Bioanal. Chem.* vol. 398, no. 1, pp. 53–66, **2010**.
- [53] I. Kariv, H. Cao, and K. R. Oldenburg, "Development of a high throughput equilibrium dialysis method," *J Pharm Sci* vol. 90, no. 5, pp. 580–587, **2001**.
- [54] M. J. Banker, T. H. Clark, J. A. Williams, "Development and validation of a 96-well equilibrium dialysis apparatus for measuring plasma protein binding," *J. Pharm. Sci.* vol. 92, no. 5, pp. 967–974, **2003**.
- [55] R. Sapin, M. D'Herbomez, J. L. Schlienger, "Free thyroxine measured with equilibrium dialysis and nine immunoassays decreases in late pregnancy," *Clin. Lab.* vol. 50, no. 9–10, pp. 581–584, **2004**.
- [56] G. Zlotos, P. Nickel, U. Holzgrabe, "Determination of protein binding of gyrase inhibitors by means of continuous ultrafiltration," *J. Pharm. Biomed. Anal.*, vol. 18, no. 3, pp. 847–858, **1998**.

- [57] J. J. Baldassare, G. M. Brenckle, M. Hoffman, F. D. Silbert, "Ultrafiltration of protein solutions; the role of protein association in rejection and osmotic pressure," *J. Membr. Sci.* vol. 31, no. 24, pp. 307–320, **1987**.
- [58] P. J. Muller, L. Hegedus, "High affinity binding of paclitaxel to human serum albumin," *Eur. J. Biochem.* vol. 268, pp. 2187–2191, **2001**.
- [59] J. Lebowitz, M. S. Lewis, P. Schuck, "Modern analytical ultracentrifugation in protein science: a tutorial review.," *Protein Sci.*, vol. 11, no. 9, pp. 2067–2079, **2002**.
- [60] J. Coleman, S. Eaton, G. Merkel, A. M. Skalka, T. Laue, "Characterization of the self association of Avian sarcoma virus integrase by analytical ultracentrifugation," *J. Biol. Chem.* vol. 274, no. 46, pp. 32842–32846, **1999**.
- [61] E. H. M. L. Heuberger, L. M. Veenhoff, R. H. Duurkens, R. H. E. Friesen, and B. Poolman, "Oligomeric state of membrane transport proteins analyzed with blue native electrophoresis and analytical ultracentrifugation.," *J. Mol. Biol.*, vol. 317, no. 4, pp. 591–600, **2002**.
- [62] A. Amini, "Recent developments in chiral capillary electrophoresis and applications of this technique to pharmaceutical and biomedical analysis," *Electrophoresis* vol. 22, no. 15, pp. 3107–3130, **2001**.
- [63] V. Pacáková, K. Štulík, S. Hubená, M. Tichá, "Affinity Capillary Electrophoresis," *Chem. List.* vol. 94, no. 2, pp. 102–104, **2000**.
- [64] I. J. Colton, J. D. Carbeck, J. Rao, G. M. Whitesides, "Affinity capillary electrophoresis: A physical-organic tool for studying interactions in biomolecular recognition," *Electrophoresis* vol. 19, no. 3, pp. 367–382, **1998**.
- [65] F. A. Gomez, L. Z. Avila, Y. H. Chu, G. M. Whitesides, "Determination of binding constants of ligands to proteins by affinity capillary electrophoresis: compensation for electroosmotic flow.," *Anal. Chem.* vol. 66, no. 11, pp. 1785–1791, **1994**.
- [66] Y. H. Chu, G. M. Whitesides, "Affinity capillary electrophoresis can simultaneously measure binding constants of multiple peptides to vancomycin," *J. Org. Chem.* vol. 57, no. 13, pp. 3524–3525, **1992**.
- [67] R. Craig, "Principles Techniques Applications Design," *Anal. Chem.* vol. 53, no. 1, pp. 20–32, **1981**.

- [68] V. Cerdà, J. M. Estela, R. Forteza, A. Cladera, E. Becerra, P. Altimira, P. Sitjar, "Flow techniques in water analysis," *Talanta* vol. 50, no. 4, pp. 695–705, **1999**.
- [69] M. E. Georgiou, C. A. Georgiou, M. A. Koupparis, "Automated flow injection gradient technique for binding studies of micromolecules to proteins using potentiometric sensors: application to bovine serum albumin with anilinonaphthalenesulfonate probe and drugs," *Anal. Chem.* vol. 71, no. 13, pp. 2541–50, **1999**.
- [70] C. D. Tran, M. S. Baptista, T. Tomooka, "Determination of binding constants by flow injection gradient technique," *Langmuir* vol. 14, no. 24, pp. 6886–6892, **1998**.
- [71] A. Majcher, A. Lewandrowska, F. Herold, J. Stefanowicz, T. Słowiński, A. P. Mazurek, S. A. Wieczorek, R. Hołyst, "A method for rapid screening of interactions of pharmacologically active compounds with albumin," *Anal. Chim. Acta*, vol. 855, pp. 51–59, **2015**.
- [72] R. Aris, "On a dispersion of a solute in a fluid flowing through a tube," *Proc. Soc. Lond.* vol. 235, no.6, pp. 67–77, **1956**.
- [73] A. Alizadeh, C.A. Nieto de Castro, W.A. Wakeham, "The theory of the Taylor Dispersion Technique for liquid diffusivity measurements," *Int. J. Thermophys.* vol. 82, no.1, pp. 243–284, **1980**.
- [74] M. Zou, Y. Han, L. Qi, Y. Chen, "Fast and accurate measurement of diffusion coefficient by Taylor's dispersion analysis," *Chinese Sci. Bull.*, vol. 52, no. 24, pp. 3325–3332, **2007**.
- [75] A. Lewandrowska, A. Majcher, A. Ochab-Marcinek, M. Tabaka, R. Hołyst, "Taylor dispersion analysis in coiled capillaries at high flow rates," *Anal. Chem.*, vol. 85, no. 8, pp. 4051–4056, **2013**.
- [76] M. Johnson, R. Kamm, "Dean number in a gently curving tube," *J. Fluid Mech.* vol.172, no. 2, pp. 329-345, **1986**.
- [77] A. Bielejewska, A. Bylina, K. Duszczyk, M. Fialkowski, R. Hołyst, "Evaluation of ligand-selector interaction from effective diffusion coefficient," *Anal. Chem.*, vol. 82, no. 13, pp. 5463–5469, **2010**.
- [78] PhD thesis, A. Zagożdżon, "Development of the Taylor dispersion method for diffusion coefficient measurements", **2016**.

- [79] M. Petrović, D. Barceló, "Determination of Anionic and Nonionic Surfactants, Their Degradation Products, and Endocrine-Disrupting Compounds in Sewage Sludge by Liquid Chromatography/Mass Spectrometry," *Anal. Chem.* vol. 72, no. 19, pp. 4560–4567, **2000**.
- [80] X. Zhang, A. Poniewierski, S. Hou, K. Sozański, A. Wisniewska, S. a. Wieczorek, T. Kalwarczyk, L. Sun, R. Hołyst, "Tracking structural transitions of bovine serum albumin in surfactant solutions by fluorescence correlation spectroscopy and fluorescence lifetime analysis," *Soft Matter* vol. 11, no. 2 pp. 2512–2518, **2015**.
- [81] B. Simončič, J. Špan, "A study of dye-surfactant interactions. Part 1. Effect of chemical structure of acid dyes and surfactants on the complex formation," *Dyes Pigments* vol. 36, no. 1, pp. 1–14, **1998**.
- [82] E. T. Soares, M. A. Lansarin, C. C. Moro, "A study of process variables for the photocatalytic degradation of rhodamine B," *Braz. J. Chem. Eng.* vol. 24, no. 1, pp. 29–36, **2007**.
- [83] H. J. Cheon, E.G. Holvey-Bates, J.W. Schoggins, S. Forster, P. Hertzog, N. Imanaka, Ch. M. Rice, M. W. Jackson, D. J. Junk, G.R. Stark, "IFN β -dependent increases in STAT1, STAT2, and IRF9 mediate resistance to viruses and DNA damage," *The EMBO Journal*. vol. 32, no. 1, pp. 2751–2763, **2013**.

B. 490/16



Biblioteka Instytutu Chemii Fizycznej PAN

F-B.490/16



90000000193897